Flower-specific jasmonate signaling regulates constitutive floral defenses in wild tobacco

Ran Li[a], Ming Wang[a], Yang Wang[a], Meredith C. Schuman[a], Arne Weinhold[a], Martin Schäfer[a], Guillermo H. Jiménez-Alemán[b], Andrea Barthel[c], and Ian T. Baldwin[a,1]

[a]Department of Molecular Ecology, Max Planck Institute for Chemical Ecology, D-07745 Jena, Germany; [b]Department of Bioorganic Chemistry, Max Planck Institute for Chemical Ecology, D-07745 Jena, Germany; and [c]Department of Entomology, Max Planck Institute for Chemical Ecology, D-07745 Jena, Germany

Edited by Sheng Yang He, Michigan State University, East Lansing, MI, and approved July 11, 2017 (received for review March 1, 2017)

Optimal defense (OD) theory predicts that within a plant, tissues are defended in proportion to their fitness value and risk of predation. The fitness value of leaves varies greatly and leaves are protected by jasmonate (JA)-inducible defenses. Flowers are vehicles of Darwinian fitness in flowering plants and are attacked by herbivores and pathogens, but how they are defended is rarely investigated. We used *Nicotiana attenuata*, an ecological model plant with well-characterized herbivore interactions to characterize defense responses in flowers. Early floral stages constitutively accumulate greater amounts of two well-characterized defensive compounds, the volatile (*E*)-α-bergamotene and trypsin proteinase inhibitors (TPIs), which are also found in herbivore-induced leaves. Plants rendered deficient in JA biosynthesis or perception by RNA interference had significantly attenuated floral accumulations of defensive compounds known to be regulated by JA in leaves. By RNA-seq, we found a JAZ gene, *NaJAZi*, specifically expressed in early-stage floral tissues. Gene silencing revealed that *NaJAZi* functions as a flower-specific jasmonate repressor that regulates JAs, (*E*)-α-bergamotene, TPIs, and a defensin. Flowers silenced in *NaJAZi* are more resistant to tobacco budworm attack, a florivore. When the defensin was ectopically expressed in leaves, performance of *Manduca sexta* larvae, a folivore, decreased. NaJAZi physically interacts with a newly identified NINJA-like protein, but not the canonical NINJA. This NINJA-like recruits the corepressor TOPLESS that contributes to the suppressive function of NaJAZi on floral defenses. This study uncovers the defensive function of JA signaling in flowers, which includes components that tailor JA signaling to provide flower-specific defense.

jasmonate signaling | jasmonate ZIM domain (JAZ) proteins | *Nicotiana attenuata* | *Manduca sexta* | *Heliothis virescens*

Plants are important sources of food and shelter in all ecosystems, and many other organisms make their livings from plants. To survive, plants have evolved sophisticated strategies to defend themselves against these attackers. The most diversified of these are the defensive compounds, which can be constitutively produced but are often induced in response to specific attackers and vary among tissues within a single plant (1, 2). Like all organisms, plants must make resource allocation decisions to optimize their Darwinian fitness. Optimal defense (OD) theory predicts that defenses are allocated to tissues in proportion to their fitness value and likelihood of attack (3, 4). The fitness value of leaves is highly stage and context specific and as the dominant aboveground component of plants, they are frequently attacked by herbivores, and defended by traits that are both constitutively and inducibly expressed (5–8). Most of these inducible defenses of leaves are regulated by attack-elicited phytohormone signaling, of which jasmonate (JA) signaling plays the dominant role (9–11). Flowers are undoubtedly among the most fitness valuable tissues of annual plants due to their intimate involvement with seed and pollen production. Moreover, flowers are nutritious and readily apparent to herbivores and hence are frequently attacked. OD theory predicts that flowers will have high levels of constitutively expressed defenses and a substantial literature that describes the species-specific secondary metabolites or defensive proteins of flowers is consistent with these predictions (12–16). In the wild tobacco, *Nicotiana attenuata*, secondary metabolites frequently accumulate in floral tissues at levels significantly higher than in leaves (2). However, little is known about how these floral defenses are regulated.

The inducible defenses of leaves are regulated by the JA phytohormones (5, 17–19). JA signaling also plays central roles in regulating other stress responses as well as several aspects of plant development (11). During flowering, JA signaling has been shown to regulate flower development and pollinator advertisement traits (20–23). However, the role of JA signaling in regulating constitutive floral defenses has not been investigated.

Both external stress factors and internal developmental signals regulate levels of JAs, especially (+)-7-*iso*-JA-Ile (JA-Ile), the bioactive form of JAs required for the activation of many responses (24). JA-Ile perception and signaling is through the F-box protein, coronatine-insensitive 1 (COI1), and JASMONATE ZIM-domain (JAZ) proteins, which form a receptor complex

Significance

Plants are at the base of most food chains and hence are frequently attacked by herbivores. Leaves are the dominant aboveground tissues of most plants and their defense responses against folivores are well studied and known to be regulated by jasmonate (JA) phytohormone signaling. As the most fitness-valuable and frequently the most nutritious tissues, flowers are also commonly attacked by florivores. However floral defense, compared with leaf defense, is rarely studied, and the signaling systems that regulate these defenses are unknown. Here we show that flowers of the wild tobacco, *Nicotiana attenuata*, constitutively accumulate large amounts of defensive compounds, trypsin proteinase inhibitors, (*E*)-α-bergamotene and defensins, and that a flower-specific sector of JA signaling regulates these constitutively expressed floral defenses.

Author contributions: R.L. and I.T.B. designed research; R.L., M.W., Y.W., A.W., M.S., G.H.J.-A., and A.B. performed research; I.T.B. contributed new reagents/analytic tools; R.L., M.W., M.C.S., and I.T.B. analyzed data; and R.L., M.C.S., and I.T.B. wrote the paper.

The authors declare no conflict of interest.

This article is a PNAS Direct Submission.

Freely available online through the PNAS open access option.

Data deposition: The sequences reported in this paper have been deposited in the GenBank database [accession nos. LOC109215118 (*NaCOI1*), LOC109240311 (*NaJAZi*), LOC109220914 (*NaJAZa*), LOC109231462 (*NaJAZb*), LOC109233155 (*NaJAZc*), LOC109226585 (*NaJAZd*), LOC109223947 (*NaJAZe*), LOC109206743 (*NaJAZf*), LOC109219395 (*NaJAZg*), LOC109215786 (*NaJAZh*), LOC109205671 (*NaJAZj*), LOC109241858 (*NaJAZk*), LOC109220335 (*NaJAZl*), LOC109211099 (*NaJAZm*), LOC109216746 (*NaNINJA*), LOC109212843 (*NaNINJA-like*), LOC109237025 (*NaTOPLESS*), LOC109232914 (*NaMYC2a*), LOC109205493 (*NaMYC2b*), LOC109206771 (*NaTPS38*), LOC109237191 (*NaDEF1*), LOC109219036 (*NaDEF2*), LOC109215124 (*NaMYB8*), and LOC109210359 (*NaPI*)]. All microarray data were deposited in the Gene Expression Omnibus (GEO) database (accession no. GSE101143).

[1]To whom correspondence should be addressed. Email: Baldwin@ice.mpg.de.

This article contains supporting information online at www.pnas.org/lookup/suppl/doi:10.1073/pnas.1703463114/-/DCSupplemental.

(25). JAZ proteins directly interact with and repress a series of JA-responsive transcription factors (TFs) (26, 27), and in the presence of JA-Ile, the SCF^{COI1} complex binds to and subsequently mediates the degradation of JAZ proteins, releasing their inhibition of downstream JA-regulated responses. The expression of JAZ genes is also known to be subsequently activated, which in part results in desensitization of JA signaling through alterative splicing variants of JAZs (28–30). This alternative splicing-mediated desensitization of JA signaling requires the N-terminal cryptic MYC-interaction domain (CMID) of JAZ, which somehow keeps JA signaling from becoming unregulated (28, 31, 32). There are at least two mechanisms required for JAZ repressor activity. The first is the interaction with the general corepressor TOPLESS (TPL). Some JAZ proteins that contain EAR motifs can directly interact with TPL (33, 34). Other JAZs that lack the EAR motif require the recruitment of an adaptor protein, NOVEL INTERACTOR OF JAZ (NINJA), which subsequently binds to TPL (35). *Arabidopsis* has a single copy of the *NINJA* gene, which is closely related to the ABI-FIVE BINDING PROTEIN (*AFP*) gene family (35). In rice, two NINJA proteins were identified to interact with OsJAZ8, which regulates bacterial blight resistance (36). These two NINJA proteins share 99% sequence similarity and hence are likely the same gene. Second, structural studies of the *Arabidopsis* MYC3 repression revealed that JAZ proteins compete with the transcriptional activator MEDIATOR25 in binding the (N)-terminal helix of MYC3 (37).

Different environmental or developmental cues may induce various outputs of JA signaling. How a single hormone governs these multiple physiological processes is a major question in the field (38). Increasingly, evidence is revealing that JA-downstream TFs mediate the specificity of JA responses. Examples include: the basic helix–loop–helix (bHLH) TF family in plant defense responses and freezing tolerance (19, 39–44); MYB TFs in stamen development, anthocyanin biosynthesis, fiber and trichome initiation (45–47); YAB TF family in anthocyanin biosynthesis (48); APETALA2 (AP2) TFs in regulation flower time (22); and WRKY TFs in senescence (49). Different JA-responsive TFs seem to be suppressed by particular JAZ proteins, suggesting that the diversity of JA responses could result from specific JAZ–TF interactions. Many studies have inferred redundant roles for JAZs in JA responses, but the functions of individual JAZ proteins remain poorly studied. Recently, a study that analyzed the expression patterns of *Arabidopsis* JAZs found a guard cell-specific AtJAZ2 to regulate the bacteria-secreted JA-Ile mimic, coronatine, which elicits stomatal reopening during bacteria invasion (50).

Here, we compared the defensive compounds found in herbivore-induced leaves with those found in different floral stages in the ecological model plant, *N. attenuata*. We asked whether JA signaling is required for floral defense in addition to its established role in developmental regulation and floral advertisement. By RNA-seq, we investigated the tissue-expression profiles of all JAZ genes in *N. attenuata*. One JAZ gene, *NaJAZi*, is specifically and highly expressed in flower tissues, particularly during early developmental stages. We asked whether *NaJAZi* specifically regulates floral JA signaling and explored the function of *NaJAZi* by the analysis of protein–protein interactions and gene silencing. Our results demonstrate that some JA-dependent defenses constitutively accumulate in flowers and that a flower-specific sector of JA signaling regulates these floral defenses and is suppressed by a NaJAZi–NINJA-like–TOPLESS complex.

Results

Early-Stage Flowers Constitutively Accumulate High Levels of (*E*)-α-Bergamotene, Trypsin Proteinase Inhibitors, and JA-Ile. To examine whether developing flowers are well defended as predicted by OD theory, we compared six defense compounds in herbivore-elicited leaves and developing flowers in *N. attenuata*. These compounds have all been shown to play important roles in the defense of leaves, and all are induced in leaves by herbivore feeding (51–55). Here we analyzed (*E*)-α-bergamotene emission 5 h after wounding and *Manduca sexta* regurgitant (W+R) treatment and the other compounds and proteins 3 d after W+R treatment in leaves, to detect maximum levels (56). Nontreated leaves at each time point served as controls. Constitutive levels of the alkaloid, nicotine, and total 17-hydroxygeranyllinalool diterpene glycosides (HGL-DTGs) were lower at all floral stages than in rosette leaves (Fig. 1 *A* and *B*). Two phenylpropanoid-polyamine conjugates, caffeoyputrescine (CP) and dicaffeoylspermidine (DCS), showed similar basal levels among different tissues, except that the levels of CP were marginally higher in early floral stages than in other tissues (Fig. 1 *C* and *D*). Remarkably, the sesquiterpene, (*E*)-α-bergamotene, and trypsin proteinase inhibitor (TPI) activity were found at substantially higher concentrations in floral tissues even compared with the high levels in herbivore-elicited leaves (Fig. 1 *E* and *F*). These results suggest that unlike leaves, developing flowers of *N. attenuata* constitutively produce specific defensive compounds such as (*E*)-α-bergamotene and TPIs to protect themselves against attackers. To evaluate whether JA signaling regulates these defense compounds in leaves, we measured JAs in different tissues and treatments. Flowers constitutively accumulated high levels of JA and jasmonoyl-isoleucine (JA-Ile) compared with the levels found in leaves (Fig. 1 *G* and *H*). One hour after W+R elicitation, JA and JA-Ile levels are known to attain maximum values in leaves (56). Remarkably, the levels of JA-Ile were 6.2-fold higher in floral stage 1 than in herbivore-elicited leaves and remained higher throughout floral development (Fig. 1*H*). These results suggested that the high levels of (*E*)-α-bergamotene and TPIs in flowers might be associated with these high JA-Ile levels.

JA Signaling Is Involved in Floral Defense. Because JA-Ile is reported to be the main bioactive JA, we asked whether JA signaling regulates the constitutive defenses of flowers. Silencing of the allene oxide cyclase (*AOC*) gene by RNA interference (RNAi) in *N. attenuata* disrupts total JA biosynthesis (57) (*SI Appendix*, Fig. S1) and silencing the F-box protein *COI1* dramatically attenuates JA perception (18); these two lines were used to address this question and the above-mentioned defense compounds mentioned were quantified in the different floral stages of these JA-deficient lines. In contrast to transgenic empty vector (EV) control plants, the amounts of nicotine, total HGL-DTGs, CP, DCS, (*E*)-α-bergamotene, and TPI were all significantly lower in floral stages 1 and 3 of inverted repeat (ir)-*aoc* and ir-*coi1* lines (Fig. 2). When flowers opened (stage 5), the levels of CP, DCS, and TPI were also significantly reduced in ir-*aoc* and ir-*coi1* lines compared with EV plants. Surprisingly, (*E*)-α-bergamotene accumulated to much higher levels in the opening stage flowers of ir-*coi1* compared with those of ir-*aoc* and EV plants (Fig. 2*E*). Because COI1 regulates the turnover of JA-Ile in leaves by negative feedback (58), the JA pool was also measured in flowers of ir-*coi1* lines. The levels of JA-Ile (1.6-fold), OH-JA-Ile (4.0-fold), COOH-JA-Ile (8.1-fold), and JA-Val (2.3-fold) were higher in floral stage 5 of ir-*coi1* lines than of EV plants (*SI Appendix*, Fig. S1 *B* and *D–F*), suggesting that the biosynthesis of (*E*)-α-bergamotene in opening-stage flowers might be regulated by COI1-independent JA signaling.

Identification of a Flower-Specific JAZ. The expression of the *JAZ* genes in different tissues may reflect their function. By mining the previously published RNA-seq data (59), the expression profiles of all JAZ genes in *N. attenuata* were extracted. In total, 13 JAZs were found in the *N. attenuata* genome (*SI Appendix*, Fig. S2*A*), and one, *NaJAZi*, was detected only in floral tissues, especially in the early developmental stage (Fig. 3*A*). Phylogenetic analysis of JAZ proteins in six plant species revealed that NaJAZi belongs to the subgroup defined by AtJAZ7, AtJAZ8, and AtJAZ13 and is most closely related to the noncanonical AtJAZ13 (*SI Appendix*, Fig. S2*A*) (33, 34). The expression profile of *NaJAZi* in different tissues was confirmed by RT-qPCR. *NaJAZi* transcripts accumulated in the early developmental stages of the gynoecium, corolla, and filament (Fig. 3*B*). To determine whether JA signaling mediates the expression of *NaJAZi* in flowers, transcripts of *NaJAZi* were

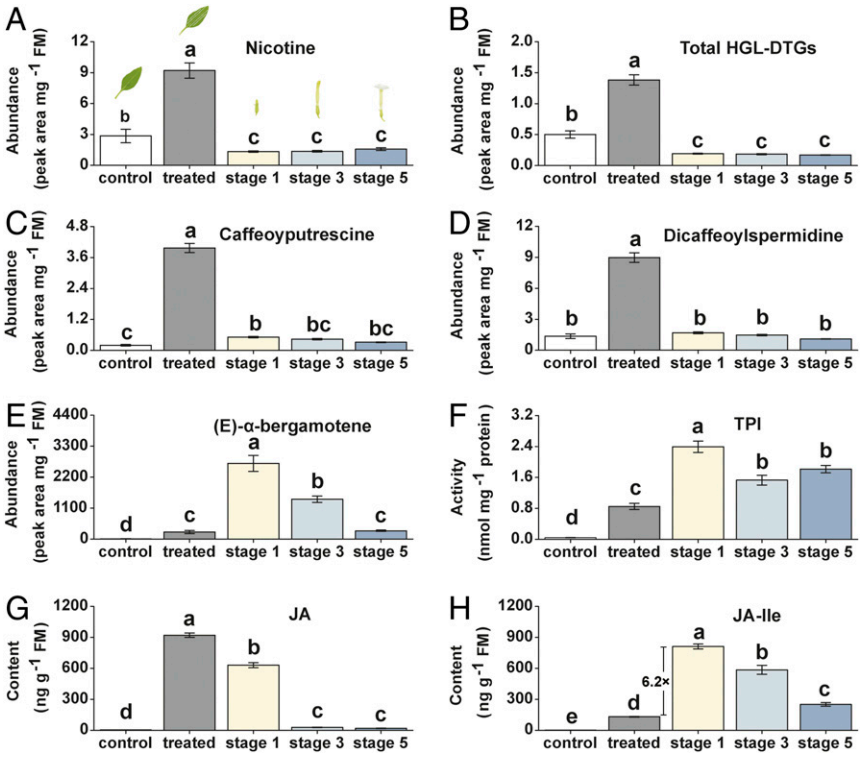

Fig. 1. Metabolites previously demonstrated to function as defenses in elicited leaves and in different flower stages. Mean nicotine (*A*), 17-hydroxygeranyllinalool diterpene glycosides (HGL-DTGs) (*B*), caffeoyputrescine (*C*), dicaffeoylspermidine (*D*), (*E*)-α-bergamotene (*E*), trypsin proteinase inhibitor (TPI) activity (*F*), JA (*G*), and JA-Ile (*H*) levels (±SE, n = 6–8) in leaves and flowers of wild-type plants. Nontreated leaves were used as control; for JA and JA-Ile measurements, leaves 1 h after wounding and treatment with *M. sexta* regurgitant (W+R) were used as treated; for (*E*)-α-bergamotene analysis, leaves 5 h after W+R treatment were used as treated; for other compounds and protein analysis, leaves 3 d after W+R treatment were used as treated; corollas emerged 0.5 cm from calyx were used as stage 1; corollas fully elongated but closed were used as stage 3; corollas opened were used as stage 5. Letters indicate significant differences among different treatments and tissues ($P < 0.05$, Duncan's multiple range test).

examined in JA-deficient lines. Relative to EV plants, *NaJAZi* transcripts were significantly lower in ir-*aoc* and ir-*coi1* lines (Fig. 3*C*).

Like other JAZ proteins, NaJAZi protein was determined to be localized in the nucleus (*SI Appendix*, Fig. S3*A*) where transcriptional suppression occurs. Moreover, JAZi has both an N-terminal TIFY domain and a C-terminal Jas domain (*SI Appendix*, Fig. S2*B*). The TIFY domain contributes to JAZ homo- and heterodimerization and the recruitment of the corepressor (38). To test the dimerization of NaJAZi, yeast two-hybrid (Y2H) assays were performed. In contrast to NaJAZb, a typical JAZ in *N. attenuata*, which forms homo- and heterodimers with itself and other JAZs, NaJAZi did not display any such interactions (*SI Appendix*, Fig. S3 *B–D*). The Gly (G) in the TIFY domain is important for JAZ dimerization: if it is substituted to Ala (A), the JAZ dimerization will be abolished (29). The TIFY domain of JAZi is a Gly-to-Ala mutant, which is consistent with the findings that JAZi cannot interact with other JAZs (*SI Appendix*, Fig. S2*B*). The Jas domain is involved in the turnover of JAZ proteins and their interactions with TFs (e.g., MYC2) (38). Interestingly, the Jas domain of NaJAZi lacks a canonical degron that may affect its interactions with COI1 in the presence of bioactive JAs (*SI Appendix*, Fig. S2*B*). Relative to NaJAZb, NaJAZi has lost the ability to interact with NaCOI1 in the present of JA-Ile or coronatine in yeast (Fig. 3*D* and *SI Appendix*, Fig. S4*A*). To determine whether JAZi is involved in COI1-dependent degradation, an in vitro degradation assay was performed. Both recombinant HIS-JAZb and HIS-JAZi proteins were rapidly degraded after incubation with crude protein from the early floral stage of EV plants, but not with crude protein treated with the proteasome inhibitor, MG132 (Fig. 3*E* and *SI Appendix*, Fig. S4 *B* and *C*). Furthermore, HIS-JAZi protein was degraded more slowly after incubation with the crude protein extract from ir-*coi1* than from EV plants, suggesting that the degradation of JAZi is partly COI1 dependent. MYC2 has been identified as a "master" regulator of plant secondary metabolism and defense responses in many species (60). *N. attenuata* has two MYC2s, which are named MYC2a and MYC2b here. The conserved helix structure in the Jas domain allows NaJAZi to bind with NaMYC2a and NaMYC2b in *N. attenuata* (Fig. 3*F* and *SI Appendix*, Fig. S2*B*).

Silencing of *NaJAZi* Increases JA Accumulations and Up-Regulates JA-Responsive Genes in Flowers. The expression of *JAZ* genes is usually rapidly induced in leaves by mechanical wounding or herbivore feeding (56, 61). *NaJAZi* transcripts were dramatically increased 1.5 h after wounding or W+R treatments (*SI Appendix*, Fig. S5*A*), but were not changed 25 h after W+R treatments (Fig. 3*A*). To clarify the function of *NaJAZi* in leaves and flowers, the expression

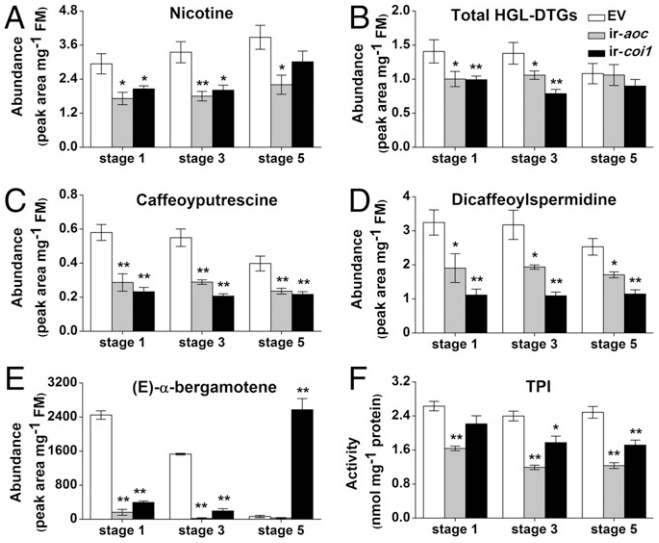

Fig. 2. Jasmonate signaling regulates levels of defense-related compounds and proteins in developing flowers. Mean nicotine (*A*), 17-hydroxygeranyllinalool diterpene glycosides (DTGs) (*B*), caffeoyputrescine (*C*) dicaffeoylspermidine (*D*), (*E*)-α-bergamotene (*E*), and trypsin proteinase inhibitor (TPI) (*F*) levels (±SE, n = 6–8) in different floral stages of empty vector (EV) control plants, inverted repeat (ir)-*aoc* plants deficient in JAs biosynthesis, and ir-*coi1* plants deficient in JA perception. Asterisks indicate significant differences in ir-*aoc*, ir-*coi1* compared with EV plants (*$P < 0.05$; **$P < 0.01$; Student's t test).

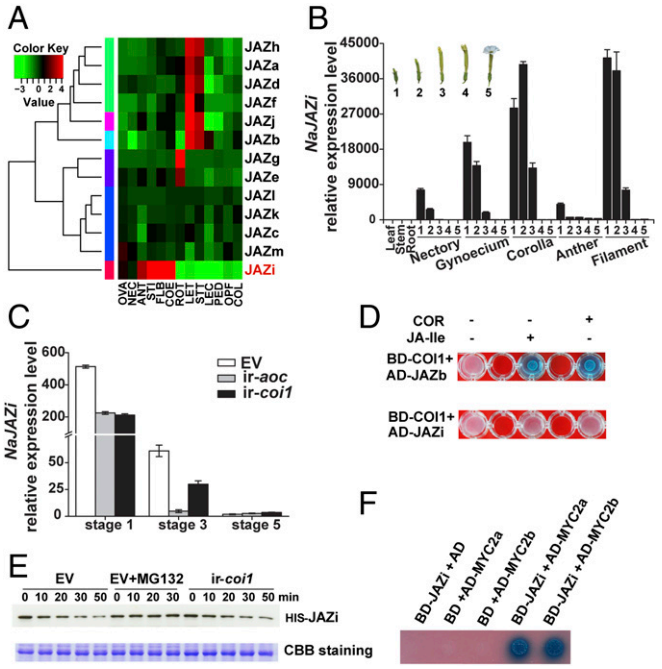

Fig. 3. Characterization of NaJAZi. (*A*) Heatmap representing the expression of JAZ genes in different tissues and treatments of *N. attenuata*. The color gradient represents the relative sequence abundance. ANT, anther; COE, corolla early; COL, corolla late; FLB, flower bud; LEC, leaf control; LET, leaf treated; NEC, nectary; OPF, opening flower; OVA, ovary; PED, pedicel; ROT, root treated; STI, stigma; STT, stem treated. Leaves 25 h after wounding and treatment with *M. sexta* regurgitant were used as treated. (*B*) Mean transcript levels (±SE, $n = 3$–5) of NaJAZi in different tissues of *N. attenuata*. (*Inset*) Five floral stages of flowers were used in this study. 1, corolla emerged 0.5 cm from calyx; 2, corolla emerged 1–2 cm from calyx; 3, corolla fully elongated but closed; 4, corolla beginning to open; and 5, corolla opened. (*C*) Mean transcripts levels (±SE, $n = 5$) of *NaJAZi* in the flowers of ir-*aoc*, ir-*coi1*, and EV plants. Flower samples from three different floral stages were analyzed. Transcript levels were analyzed by RT-qPCR. (*D*) Interaction between NaCOI1 and NaJAZ proteins by yeast two-hybrid assays. GAL4 DNA-binding domain (BD) and activation domain (AD) fusions were cotransformed into yeast strain Y2Hgold. The transformants were grown on QDO (SD −Ade/−His/−Leu/−Trp/+40 mg/L X-α-gal) plates in the presence of 50 μM coronatine (COR) or 300 μM JA-Ile or a solvent control. (*E*) In vitro JAZi degradation assays. Purified HIS–JAZi was incubated with total crude protein extracts from EV and ir-*coi1* lines; EV extract was supplemented with MG132. HIS–JAZi was detected using an anti-HIS antibody at the indicated incubation time point. The Coomassie Brilliant Blue (CBB) staining is shown as a protein loading control. (*F*) Interaction between NaJAZi and NaMYC2 proteins. BD and AD fusions were cotransformed into yeast strain Y2Hgold. The transformants were grown on QDO (SD −Ade/−His/−Leu/−Trp) plates with 40 mg/L X-α-gal.

of the *NaJAZi* gene was silenced by virus-induced gene silencing (VIGS). JAZi VIGS plants showed the same growth phenotype as the VIGS control plants in the rosette stage, but were smaller at the flowering stage. Flower morphology was not affected by *NaJAZi* silencing (*SI Appendix*, Fig. S5*B*).

First, the role of JAZi in leaves was investigated. The expression of *NaJAZi* was reduced more than 80% in leaves of JAZi VIGS plants compared with levels in control plants 1 h after W+R treatments (*SI Appendix*, Fig. S5*C*). To determine whether JA responses in leaves were altered, *M. sexta*-induced JAs and defense-related secondary metabolite levels were measured. JA and JA-Ile levels did not differ between JAZi VIGS plants and control plants after 1 h W+R treatments (*SI Appendix*, Fig. S5 *D* and *E*). Moreover, nicotine, total DTGs, and phenylpropanoid-polyamine conjugate levels were not altered by *JAZi* silencing (*SI Appendix*, Fig. S5 *F*–*I*). *M. sexta* larvae fed on JAZi VIGS plants gained a similar amount of mass compared with those that fed on control plants, suggesting that NaJAZi either did not affect JA responses in leaves or played redundant roles with other JAZs (*SI Appendix*, Fig. S5*J*).

Next, the function of NaJAZi in flowers was studied. Relative to control plants, *NaJAZi* transcripts decreased 70% on average in different floral stages of JAZi VIGS plants (Fig. 4*A*). Moreover, JAZi VIGS plants accumulated higher JA and JA-Ile levels than did control plants (Fig. 4 *B* and *C*). To evaluate the possibility of cosilencing effects, the expression of other flower-expressed JAZs was examined. Two JAZs, *NaJAZd* (1.6-fold) and *NaJAZh* (1.6-fold), were up-regulated in early floral stages of *NaJAZi*-silencing plants, whereas others showed no significant difference (*SI Appendix*, Fig. S6). Increased transcripts of *NaJAZd* and *NaJAZh* in *NaJAZi*-silenced plants may result from the high JAs levels in their flowers.

To determine whether *NaJAZi* silencing and the resulting changes in JAs would reprogram the expression of genes in flowers, microarray assays were conducted using samples from two floral stages (stages 1 and 3). Signals were considered to represent differential gene expression if there was at least a 1.5-fold change and the adjusted *P* value was less than 0.05. In total, 108 genes differed significantly between JAZi VIGS plants and VIGS control plants, 94 of which were up-regulated by *NaJAZi* silencing (*SI Appendix*, Fig. S7*A*). The expression of five selected genes in different floral stages was further confirmed by RT-qPCR and showed similar results as in the microarray data (*SI Appendix*, Fig. S7 *B*–*F*). Consistent with the observed increased JA levels in JAZi VIGS plants, many JA biosynthesis genes were found up-regulated, such as lipoxygenase (LOX5), allene oxide synthase (AOS), and amidohydrolases (ILL6 and IAR3) (Fig. 4*D* and *SI Appendix*, Fig. S7*A*). Remarkably, genes involved in terpene biosynthesis (TPSs), phenylpropanoid-polyamine conjugate biosynthesis (MYB8 and DH29), and proteinase inhibitor genes (PIs) were also all up-regulated in *NaJAZi*-silenced plants (Fig. 4*D* and *SI Appendix*, Fig. S7*A*).

Furthermore, two defensin genes (*DEF*s) showed increased transcript accumulations in JAZi VIGS plants compared with

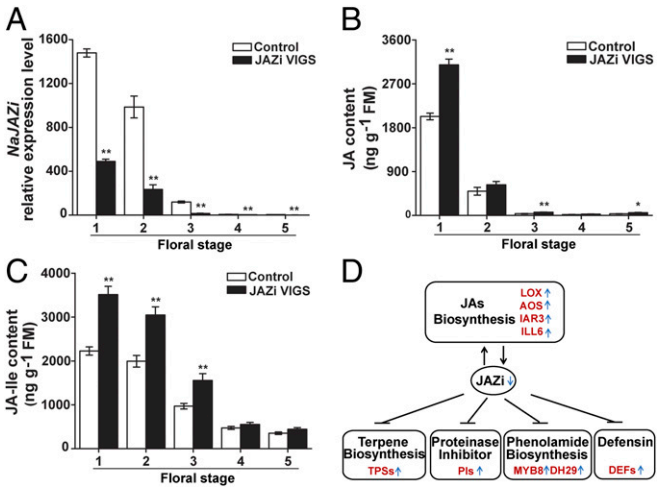

Fig. 4. Silencing of *NaJAZi* increases flower jasmonate levels and transcript accumulations of JA-related genes. (*A*) Mean transcript levels (±SE, $n = 5$) of *NaJAZi* in flowers of VIGS control and JAZi VIGS plants. Transcripts levels were analyzed by RT-qPCR. Mean JA (*B*) and JA-Ile (*C*) levels (±SE, $n = 5$) in flowers of VIGS control and JAZi VIGS plants. Samples from five different floral stages were analyzed. (*D*) Diagram represents up-regulated JA biosynthesis and responsive genes in floral stages 1 and 3 of JAZi VIGS plants compared with control plants in a microarray analysis (details of all up-regulated genes and transcript accumulation of selected genes in all floral stages are shown in *SI Appendix*, Fig. S6). Asterisks indicate significant differences in JAZi VIGS plants compared with control plants (*$P < 0.05$; **$P < 0.01$; Student's *t* test).

control plants (*SI Appendix*, Fig. S7 *E* and *F*). Plant defensins are small, cysteine-rich proteins with antimicrobial activity. Floral defensins were first identified in *Nicotiana alata* and *Petunia* plants and are thought to have antifungal activity in vitro (62, 63). The regulation of floral defensin remains unclear. Based on the transcriptional changes of *defensin* genes in *NaJAZi*-silencing plants, floral defensin might also be controlled by JA signaling. The transcriptome data suggested that JAZi mainly regulated defense responses in flowers.

Silencing of *NaJAZi* Increases Floral (*E*)-α-Bergamotene, TPI, Defensin Levels, and Resistance to Tobacco Budworm. To further evaluate whether floral defense was regulated by *NaJAZi* expression, the floral defense compounds were quantified based on the above microarray analysis. Consistent with high expression of *TPS* and *PI* genes, the levels of (*E*)-α-bergamotene and TPI activity were significantly increased in the early floral stages of *NaJAZi*-silencing plants compared with those of control plants (Fig. 5 *A* and *B*), but no differences were observed in the fully opened flowers (stage 5). Although *NaMYB8*, the key regulator of phenylpropanoid-polyamine conjugate biosynthesis, was up-regulated in *NaJAZi*-silencing plants, only CP levels, but not DCS, showed mild increases in early floral stages of JAZi VIGS plants (Fig. 5*C*). Moreover, nicotine and total HGL-DTGs levels were not changed by *NaJAZi* silencing (*SI Appendix*, Fig. S8). To evaluate whether floral defensins were also regulated by JAZi-mediated JA signaling, the protein levels of defensins were quantified in JA-deficient lines and *NaJAZi*-silenced plants. Relative to EV plants, defensin protein levels were significantly attenuated in flowers of the JA-deficient lines (Fig. 5*D* and *SI Appendix*, Fig. S9*A*). Consistent with the expression of *defensin* genes in *NaJAZi*-silencing plants (*SI Appendix*, Fig. S7 *E* and *F*), defensin protein levels were elevated in each floral stage of *NaJAZi*-silencing plants compared with those of control plants (Fig. 5*E* and *SI Appendix*, Fig. S9*B*). Structural studies of the *N. alata* floral defensin NaD1 indicated that it contains an α-amylase inhibitory activity region that was similar to the one found in VrD1, an insecticidal defensin in *Vigna radiata* (64, 65). Because *N. alata* NaD1 has high sequence similarity with NaDEF1 (80%) and NaDEF2 (100%), we inferred that these floral defensins in *N. attenuata* might also have insecticidal properties (*SI Appendix*, Fig. S10*A*). *NaDEF2* ectopic overexpression lines of *N. attenuata* (Ov*DEF2*) have been previously characterized (66) and these accumulate high levels of the DEF2 peptide in their leaves. To evaluate the insecticidal activity of NaDEF2, the performance of *M. sexta* larvae was quantified on leaves of Ov*DEF2* plants. Two independent plant lines, C230 and F278, which each harbored single T-DNA insertion, were used (*SI Appendix*, Fig. S10*B*). *M. sexta* larvae gained significantly less mass when feeding on Ov*DEF2* lines than on wild-type plants (*SI Appendix*, Fig. S10 *C* and *D*).

To determine whether the increased levels of defenses in *NaJAZi*-silenced flowers influenced the resistance of flowers to herbivores, the performance of larvae of the tobacco budworm (*Heliothis virescens*), a florivore known to prefer nicotine-deficient *N. attenuata* flowers in *N. attenuata*'s natural habitat (67), was evaluated (Fig. 5*F*). Tobacco budworm larvae gained less mass when feeding on JAZi VIGS plants than on control plants (Fig. 5*G*), demonstrating that silencing of *NaJAZi* had enhanced the resistance of flowers to tobacco budworms.

To evaluate whether other JAZs also contribute to floral defense, the function of JAZj, which showed high expression levels in flowers similar to those of JAZi, was examined using VIGS (*SI Appendix*, Fig. S11 *A* and *B* and Table S1). The expression of *DEF1* and *TPS38* was not different between *JAZj* VIGS plants and control plants (*SI Appendix*, Fig. S11 *C* and *D*), suggesting JAZj either did not affect JA responses in flower or played redundant roles with other JAZs.

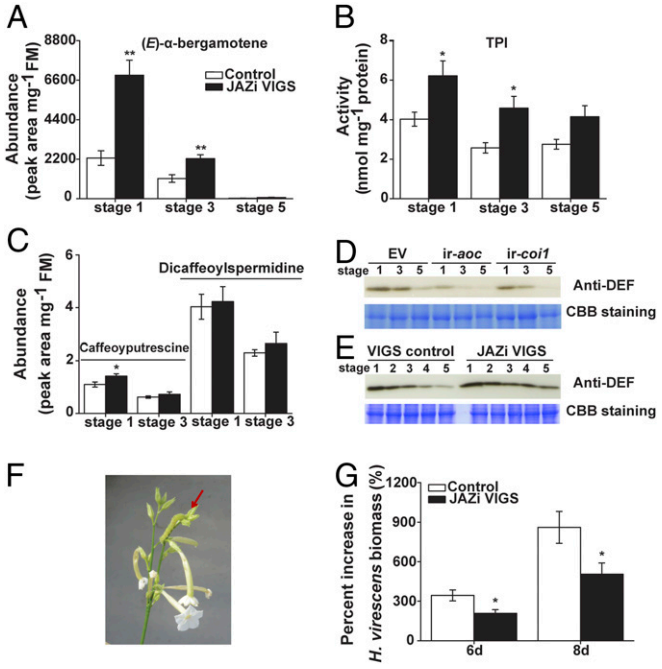

Fig. 5. Silencing of *NaJAZi* enhances jasmonate-mediated floral defense. Mean (*E*)-α-bergamotene levels (±SE, $n = 8$) (*A*), trypsin proteinase inhibitor (TPI) activity (±SE, $n = 5$) (*B*), caffeoylputrescine and dicaffeoylspermidine levels (*C*) (±SE, $n = 5$) in flowers of VIGS control and JAZi VIGS plants. (*D*) Protein levels of defensin in the flowers of ir-*aoc*, ir-*coi1*, and EV plants. (*E*) Protein levels of defensin in the flowers of VIGS control and JAZi VIGS plants. Total protein (20 μg) was used for immunoblot analysis. The Coomassie Brilliant Blue (CBB) staining is shown as a protein loading control. Flower samples from different floral stages were analyzed. (*F*) Tobacco budworm (red arrow: *H. virescens*) feeding on *N. attenuata* flowers. (*G*) Mean growth rates (±SE, $n = 15$) of individual tobacco budworm larvae that fed on VIGS control and JAZi VIGS plants. Asterisks indicate significant differences in JAZi VIGS plants compared with control plants (*$P < 0.05$; **$P < 0.01$; Student's *t* test).

NaMYC2s Regulate Floral (*E*)-α-Bergamotene, TPI, and Defensin Levels. The interaction between MYC2s and JAZi suggested JAZi-mediated floral JA responses might function directly through the suppression of MYC2s (Fig. 3*F*). To determine which floral JA responses were regulated by JAZi-MYC2s, the function of floral MYC2s was investigated by VIGS. To simultaneously silence both *MYC2a* and *MYC2b* genes, the specific fragment of MYC2a and MYC2b were ligated and used for VIGS. The transcripts of *MYC2a* and *MYC2b* were significantly decreased in MYC2 VIGS plants compared with those of VIGS control plants (Fig. 6 *A* and *B*). To determine whether MYC2s could regulate JA biosynthesis in a feedback loop, JA and JA-Ile levels were measured. JA contents were reduced by 26.4% in the early floral stage of MYC2 VIGS plants, but not in the late floral stages (Fig. 6*C*). However, the levels of bioactive JA-Ile were not changed by *MYC2s* silencing (Fig. 6*D*). Next, JAZi-mediated (*E*)-α-bergamotene, TPI, and defensin levels were examined in MYC2 VIGS plants. The TPI activity, (*E*)-α-bergamotene, and defensin levels were all significantly decreased by *MYC2* silencing (Fig. 6 *E*–*G* and *SI Appendix*, Fig. S9*C*).

NaJAZi Physically Interacts with NaNINJA-Like but Not NaNINJA. To elucidate the molecular mechanism of the suppression of floral JA responses by NaJAZi, the corepressors of NaJAZi were studied. In *Arabidopsis*, most JAZs require the adaptor protein, NINJA, to recruit the corepressor TOPLESS (35). The ortholog of *Arabidopsis* NINJA was identified in *N. attenuata*: NaNINJA. The interactions among the NaJAZs and NaNINJA were evaluated by Y2H assays. All of NaJAZs in *N. attenuata*, except for NaJAZi, could bind to NaNINJA (Fig. 7 *A* and *B*). The interaction between NaJAZg/NaNINJA or NaJAZj/NaNINJA was only observed when NaJAZg was fused with the activation domain (AD) (Fig. 7*A*) and NaJAZj was fused with the binding domain (BD) (Fig. 7*B*),

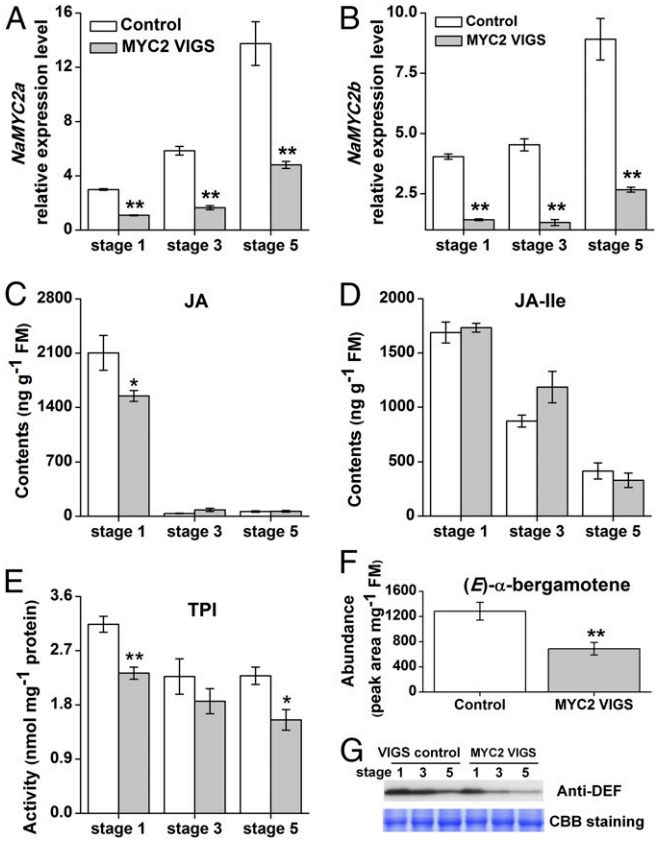

Fig. 6. Silencing of NaMYC2 attenuates jasmonate-mediated floral defenses. Mean transcript levels (±SE, $n = 5$) of *NaMYC2a* (*A*) and *NaMYC2b* (*B*) in flowers of VIGS control and MYC2 VIGS plants. Transcripts levels were analyzed by RT-qPCR. Mean JA (*C*) and JA-Ile (*D*) levels (±SE, $n = 5$) in flowers of VIGS control and MYC2 VIGS plants. Samples from three different floral stages were analyzed. (*E*) Mean trypsin proteinase inhibitor (TPI) activity (±SE, $n = 5$) in flowers of VIGS control and MYC2 VIGS plants. Samples from three different floral stages were analyzed. (*F*) Mean (*E*)-α-bergamotene levels (±SE, $n = 8$) in the early floral stage of VIGS control and MYC2 VIGS plants. (*G*) Protein levels of defensin in the flowers of VIGS control and MYC2 VIGS plants. Total protein (20 μg) was used for immunoblot analysis. The Coomassie Brilliant Blue (CBB) staining is shown as a protein loading control. Flower samples from different floral stages were analyzed.

suggesting that the activity of these JAZ proteins in yeast was affected by the fused proteins. Some JAZs containing EAR motifs are known to directly interact with TOPLESS in the absence of NINJA (33, 34); however, examination of the JAZi sequence revealed no typical EAR motifs (*SI Appendix*, Fig. S2*B*). To evaluate whether NaJAZi could directly bind to TOPLESS, the interactions among the different NaJAZs and NaTOPLESS was studied with Y2H assays. NaNINJA interacted with NaTOPLESS; however, no interactions were found among the different NaJAZs and NaTOPLESS (Fig. 7 *B* and *C*). By screening the *N. attenuata* genome, we found another gene, *NaNINJA-like*, which showed similarity with *NaNINJA* and *AtNINJA*, but not with other ABI-FIVE BINDING PROTEIN (*AFP*) genes (Fig. 7*E* and *SI Appendix*, Fig. S12). The interactions among the different NaJAZs and NaNINJA-like were then examined. Interestingly, NaNINJA-like could interact with NaJAZi and NaJAZm and weakly interacted with NaJAZk, NaJAZl, NaJAZg, and NaJAZj (Fig. 7*D*). Moreover, NaNINJA-like could also bind to TOPLESS in the Y2H assays. To confirm the interaction between NaJAZi and NaNINJA-like, in vitro pull-down assays and in vivo coimmunoprecipitation (CO-IP) assays were performed. MBP–HIS–JAZi was pulled down by GST–NINJA-like, whereas no signal was observed when GST–NINJA-like was replaced by GST or MBP–HIS–JAZi was replaced with MBP–HIS, indicating a specific NaJAZi interaction with NaNINJA-like in vitro (Fig. 7*F*). The interaction of NaJAZi and NaNINJA-like in vivo was tested using transient expression assays in *Nicotiana benthamiana* leaves. Indeed, YFP–NINJA-like but not YFP was coimmunoprecipited along with JAZi–myc (Fig. 7*G*).

NaNINJA-Like Is Involved in Floral JA Signaling. Expression profile analysis revealed that *NaNINJA-like* transcripts accumulated to levels that were fivefold higher in flower tissues than in other tissues (Fig. 8*A*). In contrast, the expression of *NaNINJA* showed no strong tissue-specific pattern (*SI Appendix*, Fig. S13). Consistent with the subcellular localization of NaJAZi, NaNINJA-like was also localized to the nucleus (Fig. 8*B*). Therefore, the formation of the JAZi–NINJA-like–TOPLESS complex suggested that NaNINJA-like might be involved in the suppressive function of NaJAZi in flowers. To address this hypothesis, the function of *NaNINJA-like* was investigated by gene silencing. The expression of *NaNINJA-like* was reduced by 45% in NaNINJA-like VIGS plants compared with that of control plants (Fig. 8*C*). The

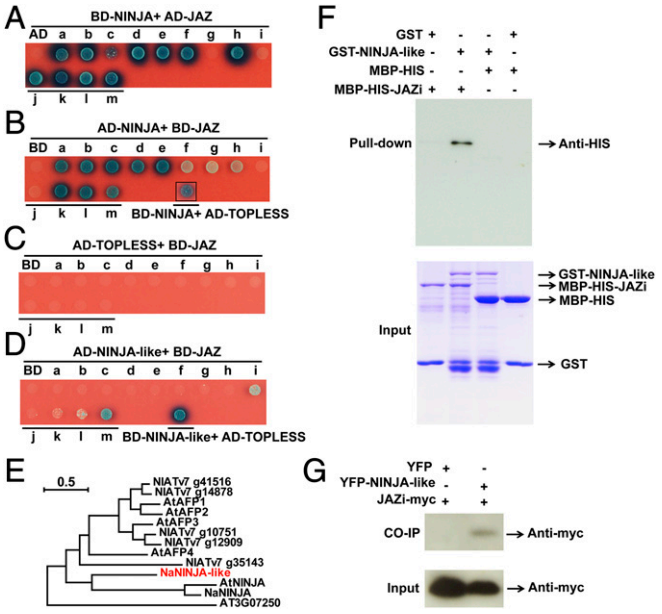

Fig. 7. Protein and protein interaction between JAZi and NINJA-like proteins. (*A*) Interaction between NINJA and JAZs by yeast two-hybrid. BD-NINJA and AD-JAZs were cotransformed into yeast strain Y2Hgold. BD-NINJA and AD cotransformed yeast were used as control. (*B*) Interaction between NINJA and JAZs by yeast two-hybrid. (*Inset*) Interaction between NINJA and TOPLESS by yeast two-hybrid. BD-JAZs/AD-NINJA or BD-NINJA/AD-TOPLESS were cotransformed into yeast strain Y2Hgold. BD- and AD-NINJA cotransformed yeast were used as control. (*C*) Interaction between TOPLESS and JAZs by yeast two-hybrid. BD-JAZs and AD-TOPLESS were cotransformed into yeast strain Y2Hgold. BD- and AD-TOPLESS cotransformed yeast were used as controls. (*D*) Interaction between NINJA-like, JAZs, and TOPLESS by yeast two-hybrid. BD-JAZs/AD-NINJA-like or BD-NINJA-like/AD-TOPLESS was cotransformed into yeast strain Y2Hgold. BD- and AD-NINJA-like cotransformed yeast were used as control. The transformants were grown on QDO (SD −Ade/−His/−Leu/−Trp) plates with 40 mg/L X-α-gal. (*E*) Phylogenetic tree analysis of ABI5 BINDING PROTEIN (ABP) in *N. attenuata* and *A. thaliana*. (*F*) In vitro pull-down assay. Two micrograms of GST or GST fusion protein was used to pull down 2 μg of HIS–MBP or HIS–MBP fusion protein. Immunoblots were performed using anti-HIS antibody to detect the associated proteins. Membranes were stained with Coomassie Brilliant Blue to monitor input protein amount. (*G*) In vivo coimmunoprecipitation assay. Protein extracts of *N. benthamiana* leaves expressing YFP–JAZi–myc or YFP–NINJA-like/JAZi–myc were immunoprecipitated with GFP-Trap_A beads. Input proteins and the immunoprecipitates were detected by anti-myc antibody.

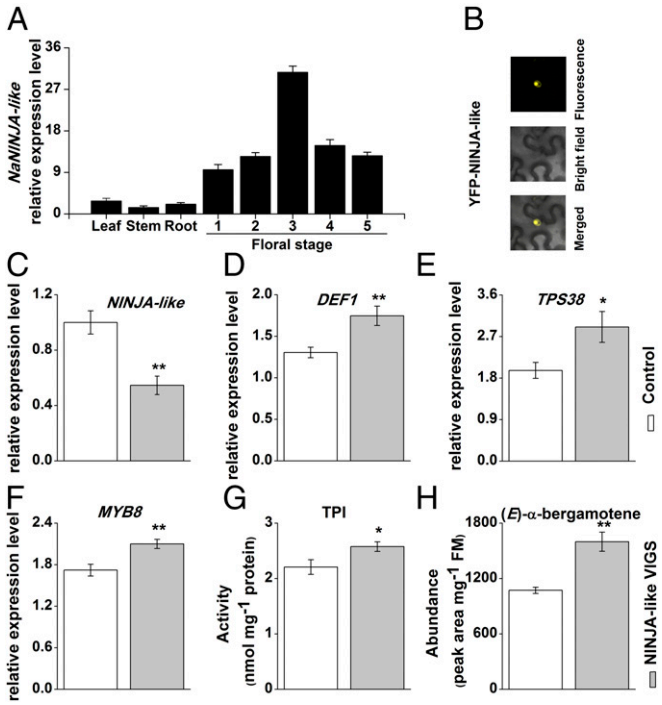

Fig. 8. Characterization of NINJA-like. (*A*) Mean transcript levels (±SE, $n = 5$) of *NaNINJA-like* in different tissues of *N. attenuata*. Transcripts levels were analyzed by RT-qPCR. (*B*) Subcellular localization of NaNINJA-like. *YFP–NINJA-like* was transiently expressed in *N. attenuata* leaves. After incubation for 48 h, the transformed cells were observed under a confocal microscope. Photographs were taken in UV light, visible light, and in their combination (merged), respectively. (Scale bar, 20 μm.) Mean transcripts levels (±SE, $n = 7$) of *NaNINJA-like* (*C*), *NaTPS38* (*D*), *NaDEF1* (*E*), and *NaMYB8* (*F*) in the flowers of VIGS control and NINJA-like VIGS plants. Transcripts levels were analyzed by RT-qPCR. Mean trypsin proteinase inhibitor (TPI) activity (±SE, $n = 5$) (*G*), and (*E*)-α-bergamotene levels (±SE, $n = 6$) (*H*) in early floral stage of VIGS control and NINJA-like VIGS plants. Asterisks indicate significant differences in NINJA-like VIGS plants compared with control plants (*$P < 0.05$; **$P < 0.01$; Student's *t* test).

expression of several NaJAZi-mediated defense-related genes was further determined in NaNINJA-like VIGS plants. As expected, the transcripts of *NaTPS38*, *NaDEF1*, and *NaMYB8* were all significantly increased in the early floral stages of NaNINJA-like VIGS plants compared with those of control plants (Fig. 8 *D*–*F*). Moreover, the levels of (*E*)-α-bergamotene and TPI activity were higher in the early floral stages of NINJA-like VIGS plants than that in VIGS control plants (Fig. 8 *G* and *H*).

Discussion

Flowers are directly required for reproduction in flowering plants, and especially in annual plants, and hence are among the most valuable tissues in terms of their contribution to Darwinian fitness. OD theory predicts that defense allocation in tissues is determined by their contribution to fitness and their probability of being attacked. Relative to defense responses in leaves, stems, and root, floral defense is rarely investigated. In nature, flowers are also attacked by pathogens and florivores. Here, we compared the defenses in different floral stages with the herbivore-induced defenses in leaves. This comparison could allow us to infer which defense compounds are involved in floral protection at specific stages. Flowers of the wild tobacco *N. attenuata* accumulate extremely high levels of (*E*)-α-bergamotene and TPI activity as part of the putative "floral arsenal" and these accumulations are most pronounced early in floral development. Like the inducible defenses of leaves, these constitutive defenses in flowers are also regulated by JA signaling but by a different sector of JA signaling than that which regulates defenses in leaves. Here we show that a single JAZ, JAZi, and its specific binding partner, NINJA-like, defined the particular sector of JA signaling that mediates the protection of this plant part that contributes so significantly to Darwinian fitness.

Nicotine, HGL-DTGs, and phenolamides are the most abundant secondary metabolites in the leaves of *N. attenuata*. However, in flowers their levels are relatively low, and in the case of nicotine, their concentrations change between day and night (68), and in nectar, nicotine occurs at highly variable and unpredictable concentrations that function to increase the outcrossing behavior of hummingbird pollinators (69). Given that high nicotine levels in flowers repel pollinators in *N. attenuata* (70), we speculate that high levels of HGL-DTGs or phenolamides in flowers might have similar effects. Other defense compounds like TPI accumulate in larger amounts in flowers than in leaves. In the flowers of tomato (*Lycopersicon esculentum*), similarly high levels of TPI were observed (14). These TPIs could inhibit gut proteinases of herbivores and might help to defend against florivores. The accumulation of defensin proteins in *N. attenuata* flowers is similar to the levels reported from *N. alata* and *Petunia* flowers (62). The antifungal activity of *N. alata* defensin has been established (63) and because insect-vectored pollination is known to increase the possibility of pathogen infection, the floral defensins of *N. attenuata* might function in pathogen resistance. When ectopically expressing *NaDEF2* in *N. attenuata* plants, leaves became more resistant to attack from *M. sexta* larvae; therefore, we infer that floral defensins in *N. attenuata* contribute to the defense of flowers against florivores.

The sesquiterpene, (*E*)-α-bergamotene, has been shown to function as an indirect defense in *N. attenuata* that attracts predators of *M. sexta*, and its production is inducibly expressed in leaves (55). We found that the flowers of *N. attenuata* constitutively accumulate (*E*)-α-bergamotene, at levels that were 10 times higher in early floral stages than in herbivore-elicited leaves (Fig. 1*E*). Although floral (*E*)-α-bergamotene is unlikely to function as an indirect defense as it does in leaves, it plays a role in attracting and guiding the behavior of pollinators in *N. attenuata* (70, 71). Interestingly, (*E*)-α-bergamotene also has been shown to have a repellent role against a nectar thief (*Solenopsis xyloni* ants) (70). Given that (*E*)-α-bergamotene is largely produced in the corolla tube (71), it might also have a defensive function in repelling other nectar robbers, such as carpenter bees (*Xylocopa* spp.), which commonly rob the nectar of flowers in *N. attenuata*'s natural habitat (67). Additional experimental work involving the release of plants silenced/overexpressing the biosynthesis genes of these putative defenses into the plant's natural habitat are required before these compounds can be rigorously considered to be defenses.

Here we demonstrated that JA signaling regulates these constitutive defenses in flowers. The regulation of JA signaling differs across tissues. In leaves, JA signaling mainly regulates inducible defense (18). In the flowers of ir-*coi1* plants, nicotine levels were 30–40% lower, whereas in leaves, they were 50% lower. For total HGL-DTGs, CP and TPI, the reductions were 16–60% in flowers but more than 80% in leaves of ir-*coi1* plants (18). Therefore, other signaling systems in addition to JA might be involved in the regulation of the constitutive defenses of flowers. In leaves or stems of *N. attenuata*, ABA, ethylene, and IAA signaling have been shown to be involved in defense responses (72–74).

JA-Ile occurs at much higher levels in flowers in different developmental stages than it does in herbivore-induced leaves, and remarkably, the amount of floral JA-Ile is greater than that of JA. JA-Ile has been shown to play an important role in corolla limb opening, floral attraction, and regulating primary metabolites in the opening flowers of *N. attenuata* (20). JA-Ile is thought to be the main bioactive JA, and levels of (*E*)-α-bergamotene, TPI, and defensin in flowers versus leaves are well correlated with the levels of JA-Ile. This correlation held in *AOC*- and *JAZi*-silenced plants. Levels of JA-Ile and (*E*)-α-bergamotene, TPI, and defensin were lower in ir-*aoc* compared with EV plants, whereas the levels of all these compounds were higher in JAZi VIGS plants compared with those of control plants. Thus, from these results one could infer that the high levels of JA-Ile serve as a ligand to promote the turnover of JAZi. However, JAZi and COI1 do not interact in

yeast in the presence of 300–2,400 μM JA-Ile or 50–400 μM coronatine. One explanation could be that the yeast system is not sufficiently sensitive to detect the interaction between JAZi and COI1. In *Arabidopsis*, the binding of JAZ8 to COI is coronatine dose dependent (33) and the flowers of *N. attenuata* can supply relatively high concentrations of JA-Ile. The results of our in vitro degradation assays suggested that the degradation of JAZi involved the 26S proteasome pathway and was somehow COI1-dependent, although the effect of COI1 is mild. Another possibility is that JAZi like other noncanonical and stable JAZs (e.g., AtJAZ8 and AtJAZ13), functions to restrain JA responses from running out of control (33, 34). The overproduction of defensive compounds in flowers could have many detrimental consequences for flower function, not only in terms of reducing outcrossing, but also in the inhibition of growth.

Combined with the results of previous studies (20), we can compile a detailed picture of the outputs of JA signaling in *N. attenuata* flowers. First, flower development, such as corolla expansion, stamen, and gynoecium maturation, is regulated by canonical JA signaling. Second, two floral traits, benzylacetone emission and nectar production important for pollinator attraction (75), are also controlled by canonical JA signaling. Third, floral defense is regulated by a specific sector of JA signaling: JAZi–MYC2-mediated regulation of defensive compounds that include (*E*)-α-bergamotene, TPI, and defensin (Figs. 5 and 6). Moreover, JAZi-dependent feedback also regulates JA levels. We hypothesize that *JAZi* silencing might activate downstream TFs, which in turn modulate the biosynthesis of JAs. In *Arabidopsis*, two auxin response TFs, ARF6 and ARF8, redundantly regulate JA biosynthesis in flower buds (76). The orthologs of ARF6 and ARF8 in *N. attenuata* are also potential targets of JAZi. Other defense compounds like nicotine might be redundantly regulated by floral-expressed JAZs. However, we still do not know whether JAZi regulates other JA responses other than the defense responses of flowers. Given that increasing JA levels in flowers does not affect flower development or the expression of pollinator attraction traits (20), we infer that the silencing of *NaJAZi* would not be a useful approach to investigate other JA signaling outputs and that experimental approaches using *JAZi* overexpression are likely to be more informative.

By investigating the suppressive function of JAZi, we identified a NINJA-like protein in *N. attenuata*. JAZi physically interacts with NINJA-like and subsequently recruits the corepressor TOPLESS. Silencing of *NINJA-like* in flowers of *N. attenuata* increased the expression of JAZi-mediated JA responsive genes, indicating that NINJA-like is involved in the suppressive function of JAZi. The phenotype of *NINJA-like* silencing is not as strong as that of *JAZi* silencing. This may result from the lower silencing efficiency of *NINJA-like* in this study or the influence of other suppressive mechanisms (37). In addition to the specific interactions between JAZi and NINJA-like, we found that JAZl and JAZm can both bind to NINJA and NINJA-like; whereas the other 10 JAZs identified in *N. attenuata* could only bind to NINJA (Fig. 7 *B* and *D*). The existence of the JAZ–NINJA or JAZ–NINJA-like complex in *N. attenuata* might enrich the diversity of JA signaling. The discovery of these NINJAs provides valuable tools for the exploration of other sectors of JA signaling. Both *JAZi* and *NINJA-like* are highly expressed in flowers; moreover, JAZi specifically interacts with NINJA-like, suggesting that NINJA-like probably coevolved with JAZi in *N. attenuata*.

This study comprehensively reveals the defensive function of JA signaling in developing flowers and provides insights into the diversity and specificity of JA signaling in plants. Given that flowers are strongly associated with Darwinian fitness, it behooves us to understand how they are defended. There remains many open questions. For example, what is the ecological function of individual defense compounds, like (*E*)-α-bergamotene, TPIs, and defensins? Is JA signaling involved in solving the flower's dilemma of defending against florivores, while at the same time attracting pollinators? Is floral JA signaling different among self-incompatible and self-pollinating species? Are other F-box proteins also involved in the perception of JA signaling? What are the functions of other JAs in flowers? Flowers provide a novel arena for exploring novel types of JA signaling, as flowers, and reproductive organs in general, are the tissues that show the greatest morphological and functional diversity among plant taxa.

Materials and Methods

Plant Material and Growth Conditions. The 31st inbred generation of *N. attenuata* derived from seeds collected at the Desert Inn Ranch in Utah in 1988 was used as the wild type. Transgenic *N. attenuata* plants silenced in the JA biosynthesis gene *AOC* (ir-*aoc*, A-07-457-1) and JA receptor *COI1* (ir-*coi1*, A-04-249-A-1) were obtained and screened as previously described (18, 57). EV transformed plants were used as transgenic control plants (67). *N. attenuata* plants overexpressing *NaDEF2* were screened as previously described (66). The single insertion lines A-09-230 (C 230) and A-09-278 (F 278) were used in this study. Wild-type *N. benthamiana* plants were used for CO-IP experiments. All of the seeds were geminated on Gamborg B5 medium as described (77). Plants for VIGS experiments and transient expression were grown in climate chambers at 20–22 °C under 16 h light. Otherwise, all plants were grown in the glasshouse with a day/light cycle of 16 h (26–28 °C)/8 h (22–24 °C) under supplemental light.

Plant Treatments and Sample Collections. For wounding (W+H_2O) treatments, leaves from rosette-stage plants were wounded with a pattern wheel, and 20 μL of distilled water was rubbed into the puncture wounds with a cleaned gloved finger; for *M. sexta* regurgitant (W+R) treatments, 20 μL of regurgitant (one-fifth diluted in distilled water) was rubbed into wounds in the same manner. Five to seven plants for each treatment were used and samples were collected at the time points indicated in *Results*. Flower sample collection was based on standardized developmental stages (see details in Fig. 3*B*). For JAs, TPI and secondary metabolites, different floral stages were harvested from three plants and pooled as one biological replicate and in total, five replicates were used. For gene expression analyses, floral tissues in different stages from 20 plants were harvest and pooled as one biological replicate and in total, three replicates were used.

Insect Performance Assay. *M. sexta* and *H. virescens* were obtained from in-house colonies at the Max Planck Institute for Chemical Ecology. One freshly hatched *M. sexta* larva was allowed to feed on each individual plant. Thirty plants of VIGS control and JAZi VIGS plants were used. Larva mass was recorded on days 9, 13, and 16. For *M. sexta* larvae performance on ov*NaDEF2* lines and WT plants, initially 20 plants of each line were used and larva mass was recorded on days 3, 6, 9, 11, and 13. For *H. virescens*, a weighed second-instar larva was used, and larva mass was recorded on days 6 and 8. The increased percentage of larval mass on each plant was calculated.

VIGS. Leaves of young *N. attenuata* plants were agroinfiltrated with pBINTRA and pTV-JAZi or pTV-JAZj or pTV-MYC2 or pTV-NINJA-like according to a published protocol optimized for VIGS in *N. attenuata* (78). Plants coinfiltrated with pBINTRA and pTV00 were used as control. All VIGS experiments were repeated at least two times.

Microarray Analysis. RNA isolated from floral stages 1 and 3 was used for microarray analysis. The 44K 60-mer oligonucleotide microarrays designed for *N. attenuata* transcriptome analysis (Agilent) were used. cDNA preparation, hybridizations, and data analysis were performed as previously described (79). Probes were filtered by 1.5-fold change and adjusted *P* values are less than 0.05.

Y2H Assay. Y2H was performed using Matchmaker Gold Yeast Two-Hybrid System (Clontech) according to the manufacturer's manual. Indicated AD and BD control or fusion constructs were cotransformed into yeast strain Y2Hgold and plated on SD −Leu/−Trp selective dropout medium. The transformations grew on QDO (SD −Ade/−His/−Leu/−Trp) plates in the present of 40 mg/L X-α-gal at 30 °C. For COI1-JAZ transformations, the plate was additionally supplemented with 50–400 μM coronatine or 300–2,400 μM JA-Ile. The plate was photographed 5–7 d after incubation.

JA Analysis. Approximately 50 mg material was used for JA analysis. Samples from JA-deficient lines and EV plants were extracted as previously described (80). For other samples, 800 μL ethylacetate containing the internal standards (10 ng D4-ABA, 10 ng D6-JA, 10 ng D6-JA-Ile, and 10 ng D6-SA) was added and mixed using a Genogrinder (SPEX Certi Prep) at a frequency of 1,000 strokes per minute for 1 min. The extractions were centrifuged at 13,200 rpm at 4 °C for 20 min. The supernatant was transferred to a new vial

and evaporated at 45 °C under a constant nitrogen stream until dryness. The extracts were dissolved in 300 μL 70% MeOH. All samples were analyzed by UHPLC-HESI-MS/MS as previously described (78).

Volatile Analysis. The emission of (*E*)-α-bergamotene from leaves and flowers was sampled using polydimethylsiloxane (PDMS) (Roth) tubes as described (81). A new fully expanded leaf was treated by W+R for 5 h and immediately enclosed into a 650-mL ventilated PET container with one PDMS tube. After 1 h of exposure, PDMS tubes were collected. For floral volatile experiments, flowers were excised and placed into a 15-mL glass vial (Sigma) with one PDMS tube at the bottom. After 1 h trapping, the PDMS tube was collected. The volatiles were analyzed by TD-20 thermal desorption unit (Shimazu) connected to a gas chromatograph quadruple mass spectrometer (GC-MS-QP2010Ultra, Shimazu). Four flowers from stage 1 or two flowers from stages 3 and 5 were used for one trapping; in total eight replicates were performed for each experiment.

TPI Analysis. Approximately 100 mg of material was homogenized with 300 μL of cold extraction buffer (0.1 M Tris-C1, pH 7.6, 5% polyvinylpolypyrrolidone, 2 mg/mL phenylthiourea, 5 mg/mL diethyldithiocarbamate, 0.05 M Na2EDTA). TPI activity was measured using a radial diffusion assay as described previously (82).

Analysis of Secondary Metabolites by HPLC. Approximately 50 mg of material was extracted using 800 μL 80% MeOH and extracts were analyzed by an ESI-TOF mass spectrometer (Bruker Daltonic) as previously described (83).

Defensin Analysis. Flower material was ground and homogenized with an extraction buffer (0.1 M Tris-C1, pH 7.6; 5% polyvinylpolypyrrolidone, 2 mg/mL phenylthiourea, 5 mg/mL diethyldithiocarbamate, 0.05 M Na_2EDTA). A total of 30 μg of total protein was used for SDS/PAGE analysis. After electrophoresis, the gels were stained with Coomassie Brilliant Blue or subjected to immunoblot analysis using an anti-defensin antibody. Antibody with specificity to flowers DEF1 and DEF2 was generated by immunizing rabbits with the peptide GRCSKILRR and purified by the GenScript.

Quantitative RT-PCR. Total RNA was isolated using the RNeasy Plant Mini Kit (Qiagen), and 800 ng of total RNA for each sample was reverse transcribed using the PrimeScript RT-qPCR Kit (TaKaRa). Three to eight independent biological samples were collected and analyzed. RT-qPCR was performed on the Stratagene 500 MX3005P using a SYBR Green reaction mix (Eurogentec). The primers used for mRNA detection of target genes by RT-qPCR are listed in *SI Appendix*, Table S2. The *N. attenuata IF5a-2* mRNA were used as internal control.

Constructs. Full-length ORFs encoding JAZa-m, MYC2a, MYC2b, COI1, NINJA, NINJA like, and TOPLESS without a stop codon were amplified by PCR using *Pfu* DNA polymerase (Thermo Scientific) with primers listed in *SI Appendix*, Table S2. For Y2H assays, each JAZ, NINJA, and COI1 were cloned into pGBKT7 to generate BD fused constructs; each JAZ, NINJA, NINJA-like, MYC2a, MYC2b, and TOPLESS were cloned into pGADT7 to generate AD fused genes. For transient expression experiments, JAZi was cloned into pBA-YFP and pEarleyGate 203 to generate C-terminal YFP fused and C-terminal myc fused gene, respectively; NINJA-like was cloned into pEarleyGate 104 to generate N-terminal YFP fused gene. Constructs were transformed into *Agrobacterium tumefaciens* GV3101. For prokaryotic expression, JAZi and NINJA-like were cloned into pDEST–N112–MBP and pDEST15 to generate HIS–MBP and GST fused gene, respectively. Constructs were transformed into *Escherichia coli* BL21 (DE3). For VIGS experiments, ~300-bp mRNA sequences of JAZi, JAZj, MYC2a, MYC2b, and NINJA-like were amplified by PCR using *Pfu* DNA polymerase (Thermo Scientific) with primers listed in *SI Appendix*, Table S2. Fragments of NaMYC2a and NaMYC2b were ligated by another round of PCR using the forward primer of MYC2a and reverse primer of MYC2b. The DNA fragments were cloned into pTV00 and transformed into *A. tumefaciens* GV3101.

Subcellular Localization. *Agrobacterium* containing 35S: *JAZi-YFP* or 35S: *YFP* or 35S: *YFP–NINJA-like* construct was infiltrated into *N. attenuata* leaves. Two days after incubation, fluorescence was analyzed by confocal microscopy.

Purification of Recombinant Protein. The overnight culture containing HIS–MBP–JAZi and GST–NINJA-like constructs were transferred to 500 mL Luria-Bertani (LB) medium with 100 mg/L amplicillin and incubated to OD_{600} 0.5 at 37 °C. The expression was induced by adding 0.4 mM isopropyl-β-thio-galactopyranoside (IPTG) for an additional 3 h at 37 °C. HIS-tagged protein was purified using Ni-NTA agarose (Qiagen) according to manufacturer's instructions. GST-tagged protein was purified using glutathione Sepharose 4B (GE Healthcare) according to manufacturer's instructions.

In Vitro Pull-Down Assay. Pull-down assays were performed as described previously (84); 2 μg of GST-tagged NINJA-like and 2 μg of HIS–MBP-tagged JAZi were used. The samples were analyzed by SDS/PAGE. After electrophoresis, the gels were stained with Coomassie Brilliant Blue or subjected to immunoblot analysis using anti-HIS antibody.

In Vitro JAZ Degradation Assay. HIS–JAZb and HIS–JAZi degradation assays were performed as described (85). Flowers in the early floral stage of each genotype were used for crude protein extraction. The incubation was conducted at room temperature.

Co-Immunoprecipitation Assay. *N. benthamiana* leaves were coinfiltrated with *Agrobacterium* containing genes encoding *JAZi–myc/YFP–NINJA-like*, or *JAZi–myc/YFP*. Leaves were harvested after a 48-h incubation at 25 °C. Total proteins of 5-g leaf samples were extracted in 2.5 mL lysis buffer [150 μM NaCl, 10% glyceol, 1 mM EDTA, 50 mM Tris·HCl (PH 7.5), 0.5% Nonidet P-40, 2 mM DTT, 1 mM PMSF and a protease inhibitor mixture]. A total of 250 μL GFP-Trap_A beads (Chromotek) was added into the extraction and incubated at 4 °C for 3 h. After being washed three times by a washing buffer [150 μM NaCl, 1 mM EDTA, 50 mM Tris·HCl (PH 7.5), 0.5% Nonidet P-40], the beads were suspended in 50 μL 2× SDS loading buffer and heated at 95 °C for 5 min. A total of 20 μL of immunoprecipitant was separated by SDS/PAGE and immunoblotted using anti-myc antibody.

Additional Accession Numbers. The other gene accession numbers not originating from our research and paper can be found in *SI Appendix*, Table S3.

ACKNOWLEDGMENTS. We thank the glasshouse team of Max Planck Institute for Chemical Ecology for plant cultivation; Evan Braithwaite, Dapeng Li, Suhua Li, Wenwu Zhou, Klaus Gase, Rayko Halitschke, and Eva Rothe for technical assistance; and Shuqing Xu and Jianqiang Wu for fruitful discussions. This work was supported by the Max Planck Society, the European Research Council Advanced Grant ClockworkGreen (293926) (to I.T.B.), the Collaborative Research Centre Chemical Mediators in Complex Biosystems-ChemBioSys (CRC 1127) funded by the German Research Foundation, and by a Humboldt Postdoctoral Research Fellowship (to R.L.).

1. Schuman MC, Baldwin IT (2016) The layers of plant responses to insect herbivores. *Annu Rev Entomol* 61:373–394.
2. Li D, Heiling S, Baldwin IT, Gaquerel E (2016) Illuminating a plant's tissue-specific metabolic diversity using computational metabolomics and information theory. *Proc Natl Acad Sci USA* 113:E7610–E7618.
3. McKey D (1974) Adaptive patterns in alkaloid physiology. *Am Nat* 108:305–320.
4. McKey D (1979) The distribution of secondary compounds within plants. *Herbivores: Their Interaction with Secondary Plant Metabolites* (Academic, New York), pp 55–133.
5. Farmer EE (2014) *Leaf Defence* (Oxford Univ Press, Oxford).
6. Ohnmeiss TE, Baldwin IT (2000) Optimal defense theory predicts the ontogeny of an induced nicotine defense. *Ecology* 81:1765–1783.
7. Karban R, Baldwin IT (2007) *Induced Responses to Herbivory* (University of Chicago Press, Chicago).
8. Walters D (2011) *Plant Defense: Warding Off Attack by Pathogens, Herbivores and Parasitic Plants* (John Wiley & Sons, Malden, MA).
9. Wu J, Baldwin IT (2010) New insights into plant responses to the attack from insect herbivores. *Annu Rev Genet* 44:1–24.
10. Howe GA, Jander G (2008) Plant immunity to insect herbivores. *Annu Rev Plant Biol* 59:41–66.
11. Wasternack C, Hause B (2013) Jasmonates: Biosynthesis, perception, signal transduction and action in plant stress response, growth and development. An update to the 2007 review in Annals of Botany. *Ann Bot (Lond)* 111:1021–1058.
12. Alves MN, Sartoratto A, Trigo JR (2007) Scopolamine in *Brugmansia suaveolens* (Solanaceae): Defense, allocation, costs, and induced response. *J Chem Ecol* 33:297–309.
13. Çirak C, Radusiene J, Janulis V, Ivanauskas L (2008) Pseudohypericin and hyperforin in *Hypericum perforatum* from Northern Turkey: Variation among populations, plant parts and phenological stages. *J Integr Plant Biol* 50:575–580.
14. Damle MS, Giri AP, Sainani MN, Gupta VS (2005) Higher accumulation of proteinase inhibitors in flowers than leaves and fruits as a possible basis for differential feeding preference of *Helicoverpa armigera* on tomato (*Lycopersicon esculentum* Mill, Cv. Dhanashree). *Phytochemistry* 66:2659–2667.
15. Fordyce JA (2000) A model without a mimic: Aristolochic acids from the California pipevine swallowtail, *Battus philenor hirsuta*, and its host plant, *Aristolochia californica*. *J Chem Ecol* 26:2567–2578.

16. Frölich C, Ober D, Hartmann T (2007) Tissue distribution, core biosynthesis and diversification of pyrrolizidine alkaloids of the lycopsamine type in three Boraginaceae species. *Phytochemistry* 68:1026–1037.
17. Halitschke R, Baldwin IT (2003) Antisense *LOX* expression increases herbivore performance by decreasing defense responses and inhibiting growth-related transcriptional reorganization in *Nicotiana attenuata*. *Plant J* 36:794–807.
18. Paschold A, Halitschke R, Baldwin IT (2007) Co(i)-ordinating defenses: NaCOI1 mediates herbivore- induced resistance in *Nicotiana attenuata* and reveals the role of herbivore movement in avoiding defenses. *Plant J* 51:79–91.
19. Schweizer F, et al. (2013) Arabidopsis basic helix-loop-helix transcription factors MYC2, MYC3, and MYC4 regulate glucosinolate biosynthesis, insect performance, and feeding behavior. *Plant Cell* 25:3117–3132.
20. Stitz M, Hartl M, Baldwin IT, Gaquerel E (2014) Jasmonoyl-L-isoleucine coordinates metabolic networks required for anthesis and floral attractant emission in wild tobacco (*Nicotiana attenuata*). *Plant Cell* 26:3964–3983.
21. Yuan Z, Zhang D (2015) Roles of jasmonate signalling in plant inflorescence and flower development. *Curr Opin Plant Biol* 27:44–51.
22. Zhai Q, et al. (2015) Transcriptional mechanism of jasmonate receptor COI1-mediated delay of flowering time in Arabidopsis. *Plant Cell* 27:2814–2828.
23. Sherif S, et al. (2015) A stable JAZ protein from peach mediates the transition from outcrossing to self-pollination. *BMC Biol* 13:11.
24. Fonseca S, et al. (2009) (+)-7-iso-Jasmonoyl-L-isoleucine is the endogenous bioactive jasmonate. *Nat Chem Biol* 5:344–350.
25. Sheard LB, et al. (2010) Jasmonate perception by inositol-phosphate-potentiated COI1-JAZ co-receptor. *Nature* 468:400–405.
26. Chini A, et al. (2007) The JAZ family of repressors is the missing link in jasmonate signalling. *Nature* 448:666–671.
27. Thines B, et al. (2007) JAZ repressor proteins are targets of the SCF(^{COI1}) complex during jasmonate signalling. *Nature* 448:661–665.
28. Moreno JE, et al. (2013) Negative feedback control of jasmonate signaling by an alternative splice variant of JAZ10. *Plant Physiol* 162:1006–1017.
29. Chung HS, Howe GA (2009) A critical role for the TIFY motif in repression of jasmonate signaling by a stabilized splice variant of the JASMONATE ZIM-domain protein JAZ10 in Arabidopsis. *Plant Cell* 21:131–145.
30. Chung HS, et al. (2010) Alternative splicing expands the repertoire of dominant JAZ repressors of jasmonate signaling. *Plant J* 63:613–622.
31. Goossens J, Swinnen G, Vanden Bossche R, Pauwels L, Goossens A (2015) Change of a conserved amino acid in the MYC2 and MYC3 transcription factors leads to release of JAZ repression and increased activity. *New Phytol* 206:1229–1237.
32. Zhang F, et al. (2017) Structural insights into alternative splicing-mediated desensitization of jasmonate signaling. *Proc Natl Acad Sci USA* 114:1720–1725.
33. Shyu C, et al. (2012) JAZ8 lacks a canonical degron and has an EAR motif that mediates transcriptional repression of jasmonate responses in Arabidopsis. *Plant Cell* 24:536–550.
34. Thireault C, et al. (2015) Repression of jasmonate signaling by a non-TIFY JAZ protein in Arabidopsis. *Plant J* 82:669–679.
35. Pauwels L, et al. (2010) NINJA connects the co-repressor TOPLESS to jasmonate signalling. *Nature* 464:788–791.
36. Yamada S, et al. (2012) Involvement of OsJAZ8 in jasmonate-induced resistance to bacterial blight in rice. *Plant Cell Physiol* 53:2060–2072.
37. Zhang F, et al. (2015) Structural basis of JAZ repression of MYC transcription factors in jasmonate signalling. *Nature* 525:269–273.
38. Chini A, Gimenez-Ibanez S, Goossens A, Solano R (2016) Redundancy and specificity in jasmonate signalling. *Curr Opin Plant Biol* 33:147–156.
39. Goossens J, Mertens J, Goossens A (2017) Role and functioning of bHLH transcription factors in jasmonate signalling. *J Exp Bot* 68:1333–1347.
40. Zhang HB, Bokowiec MT, Rushton PJ, Han SC, Timko MP (2012) Tobacco transcription factors NtMYC2a and NtMYC2b form nuclear complexes with the NtJAZ1 repressor and regulate multiple jasmonate-inducible steps in nicotine biosynthesis. *Mol Plant* 5:73–84.
41. Shoji T, Hashimoto T (2011) Tobacco MYC2 regulates jasmonate-inducible nicotine biosynthesis genes directly and by way of the NIC2-locus ERF genes. *Plant Cell Physiol* 52:1117–1130.
42. Nakata M, et al. (2013) A bHLH-type transcription factor, ABA-INDUCIBLE BHLH-TYPE TRANSCRIPTION FACTOR/JA-ASSOCIATED MYC2-LIKE1, acts as a repressor to negatively regulate jasmonate signaling in arabidopsis. *Plant Cell* 25:1641–1656.
43. Song S, et al. (2013) The bHLH subgroup IIId factors negatively regulate jasmonate-mediated plant defense and development. *PLoS Genet* 9:e1003653.
44. Hu Y, Jiang L, Wang F, Yu D (2013) Jasmonate regulates the inducer of cbf expression-C-repeat binding factor/DRE binding factor1 cascade and freezing tolerance in Arabidopsis. *Plant Cell* 25:2907–2924.
45. Song S, et al. (2011) The Jasmonate-ZIM domain proteins interact with the R2R3-MYB transcription factors MYB21 and MYB24 to affect Jasmonate-regulated stamen development in Arabidopsis. *Plant Cell* 23:1000–1013.
46. Qi T, et al. (2011) The Jasmonate-ZIM-domain proteins interact with the WD-Repeat/bHLH/MYB complexes to regulate Jasmonate-mediated anthocyanin accumulation and trichome initiation in *Arabidopsis thaliana*. *Plant Cell* 23:1795–1814.
47. Hu H, et al. (2016) GhJAZ2 negatively regulates cotton fiber initiation by interacting with the R2R3-MYB transcription factor GhMYB25-like. *Plant J* 88:921–935.
48. Boter M, et al. (2015) FILAMENTOUS FLOWER is a direct target of JAZ3 and modulates responses to jasmonate. *Plant Cell* 27:3160–3174.
49. Jiang Y, Liang G, Yang S, Yu D (2014) Arabidopsis WRKY57 functions as a node of convergence for jasmonic acid- and auxin-mediated signaling in jasmonic acid-induced leaf senescence. *Plant Cell* 26:230–245.
50. Gimenez-Ibanez S, et al. (2017) JAZ2 controls stomata dynamics during bacterial invasion. *New Phytol* 213:1378–1392.
51. Heiling S, et al. (2010) Jasmonate and ppHsystemin regulate key Malonylation steps in the biosynthesis of 17-Hydroxygeranyllinalool Diterpene Glycosides, an abundant and effective direct defense against herbivores in *Nicotiana attenuata*. *Plant Cell* 22:273–292.
52. Steppuhn A, Gase K, Krock B, Halitschke R, Baldwin IT (2004) Nicotine's defensive function in nature. *PLoS Biol* 2:E217.
53. Kaur H, Heinzel N, Schöttner M, Baldwin IT, Gális I (2010) R2R3-NaMYB8 regulates the accumulation of phenylpropanoid-polyamine conjugates, which are essential for local and systemic defense against insect herbivores in *Nicotiana attenuata*. *Plant Physiol* 152:1731–1747.
54. Zavala JA, Patankar AG, Gase K, Hui D, Baldwin IT (2004) Manipulation of endogenous trypsin proteinase inhibitor production in *Nicotiana attenuata* demonstrates their function as antiherbivore defenses. *Plant Physiol* 134:1181–1190.
55. Kessler A, Baldwin IT (2001) Defensive function of herbivore-induced plant volatile emissions in nature. *Science* 291:2141–2144.
56. Oh Y, Baldwin IT, Gális I (2012) NaJAZh regulates a subset of defense responses against herbivores and spontaneous leaf necrosis in *Nicotiana attenuata* plants. *Plant Physiol* 159:769–788.
57. Kallenbach M, Bonaventure G, Gilardoni PA, Wissgott A, Baldwin IT (2012) Empoasca leafhoppers attack wild tobacco plants in a jasmonate-dependent manner and identify jasmonate mutants in natural populations. *Proc Natl Acad Sci USA* 109: E1548–E1557.
58. Paschold A, Bonaventure G, Kant MR, Baldwin IT (2008) Jasmonate perception regulates jasmonate biosynthesis and JA-Ile metabolism: The case of COI1 in *Nicotiana attenuata*. *Plant Cell Physiol* 49:1165–1175.
59. Brockmöller T, et al. (2017) *Nicotiana attenuata* Data Hub (NaDH): An integrative platform for exploring genomic, transcriptomic and metabolomic data in wild tobacco. *BMC Genomics* 18:79.
60. Kazan K, Manners JM (2013) MYC2: The master in action. *Mol Plant* 6:686–703.
61. Chung HS, et al. (2008) Regulation and function of Arabidopsis JASMONATE ZIM-domain genes in response to wounding and herbivory. *Plant Physiol* 146:952–964.
62. Lay FT, Brugliera F, Anderson MA (2003) Isolation and properties of floral defensins from ornamental tobacco and petunia. *Plant Physiol* 131:1283–1293.
63. Dracatos PM, et al. (2014) Inhibition of cereal rust fungi by both class I and II defensins derived from the flowers of *Nicotiana alata*. *Mol Plant Pathol* 15:67–79.
64. Lin KF, et al. (2007) Structure-based protein engineering for α-amylase inhibitory activity of plant defensin. *Proteins* 68:530–540.
65. Poon IKh, et al. (2014) Phosphoinositide-mediated oligomerization of a defensin induces cell lysis. *Elife* 3:e01808.
66. Weinhold A, Wielsch N, Svatoš A, Baldwin IT (2015) Label-free nanoUPLC-MSE based quantification of antimicrobial peptides from the leaf apoplast of *Nicotiana attenuata*. *BMC Plant Biol* 15:18.
67. Kessler D, Gase K, Baldwin IT (2008) Field experiments with transformed plants reveal the sense of floral scents. *Science* 321:1200–1202.
68. Euler M, Baldwin IT (1996) The chemistry of defense and apparency in the corollas of *Nicotiana attenuata*. *Oecologia* 107:102–112.
69. Kessler D, et al. (2012) Unpredictability of nectar nicotine promotes outcrossing by hummingbirds in *Nicotiana attenuata*. *Plant J* 71:529–538.
70. Kessler D, Baldwin IT (2007) Making sense of nectar scents: The effects of nectar secondary metabolites on floral visitors of *Nicotiana attenuata*. *Plant J* 49:840–854.
71. Zhou W, et al. (2017) Tissue-specific emission of (E)-α-bergamotene helps resolve the dilemma when pollinators are also herbivores. *Curr Biol* 27:1336–1341.
72. Dinh ST, Baldwin IT, Galis I (2013) The HERBIVORE ELICITOR-REGULATED1 gene enhances abscisic acid levels and defenses against herbivores in *Nicotiana attenuata* plants. *Plant Physiol* 162:2106–2124.
73. Machado RA, et al. (2016) Auxin is rapidly induced by herbivory attack and regulates systemic, jasmonate-dependent defenses. *Plant Physiol* 172:521–532.
74. von Dahl CC, et al. (2007) Tuning the herbivore-induced ethylene burst: The role of transcript accumulation and ethylene perception in *Nicotiana attenuata*. *Plant J* 51:293–307.
75. Kessler D, et al. (2015) How scent and nectar influence floral antagonists and mutualists. *eLife* 4:e07641.
76. Nagpal P, et al. (2005) Auxin response factors ARF6 and ARF8 promote jasmonic acid production and flower maturation. *Development* 132:4107–4118.
77. Krügel T, Lim M, Gase K, Halitschke R, Baldwin IT (2002) Agrobacterium-mediated transformation of *Nicotiana attenuata*, a model ecological expression system. *Chemoecology* 12:177–183.
78. Saedler R, Baldwin IT (2004) Virus-induced gene silencing of jasmonate-induced direct defences, nicotine and trypsin proteinase-inhibitors in *Nicotiana attenuata*. *J Exp Bot* 55:151–157.
79. Zhou W, et al. (2016) Evolution of herbivore-induced early defense signaling was shaped by genome-wide duplications in *Nicotiana*. *Elife* 5:e19531.
80. Schäfer M, Brütting C, Baldwin IT, Kallenbach M (2016) High-throughput quantification of more than 100 primary- and secondary-metabolites, and phytohormones by a single solid-phase extraction based sample preparation with analysis by UHPLC-HESI-MS/MS. *Plant Methods* 12:30.
81. Kallenbach M, et al. (2014) A robust, simple, high-throughput technique for time-resolved plant volatile analysis in field experiments. *Plant J* 78:1060–1072.
82. van Dam NM, Horn M, Mareš M, Baldwin IT (2001) Ontogeny constrains systemic protease inhibitor response in *Nicotiana attenuata*. *J Chem Ecol* 27:547–568.
83. Kim SG, Yon F, Gaquerel E, Gulati J, Baldwin IT (2011) Tissue specific diurnal rhythms of metabolites and their regulation during herbivore attack in a native tobacco, *Nicotiana attenuata*. *PLoS One* 6:e26214.
84. Li R, et al. (2014) Virulence factors of geminivirus interact with MYC2 to subvert plant resistance and promote vector performance. *Plant Cell* 26:4991–5008.
85. Wu D, et al. (2017) Viral effector protein manipulates host hormone signaling to attract insect vectors. *Cell Res* 27:402–415.

Supporting Information Appendix

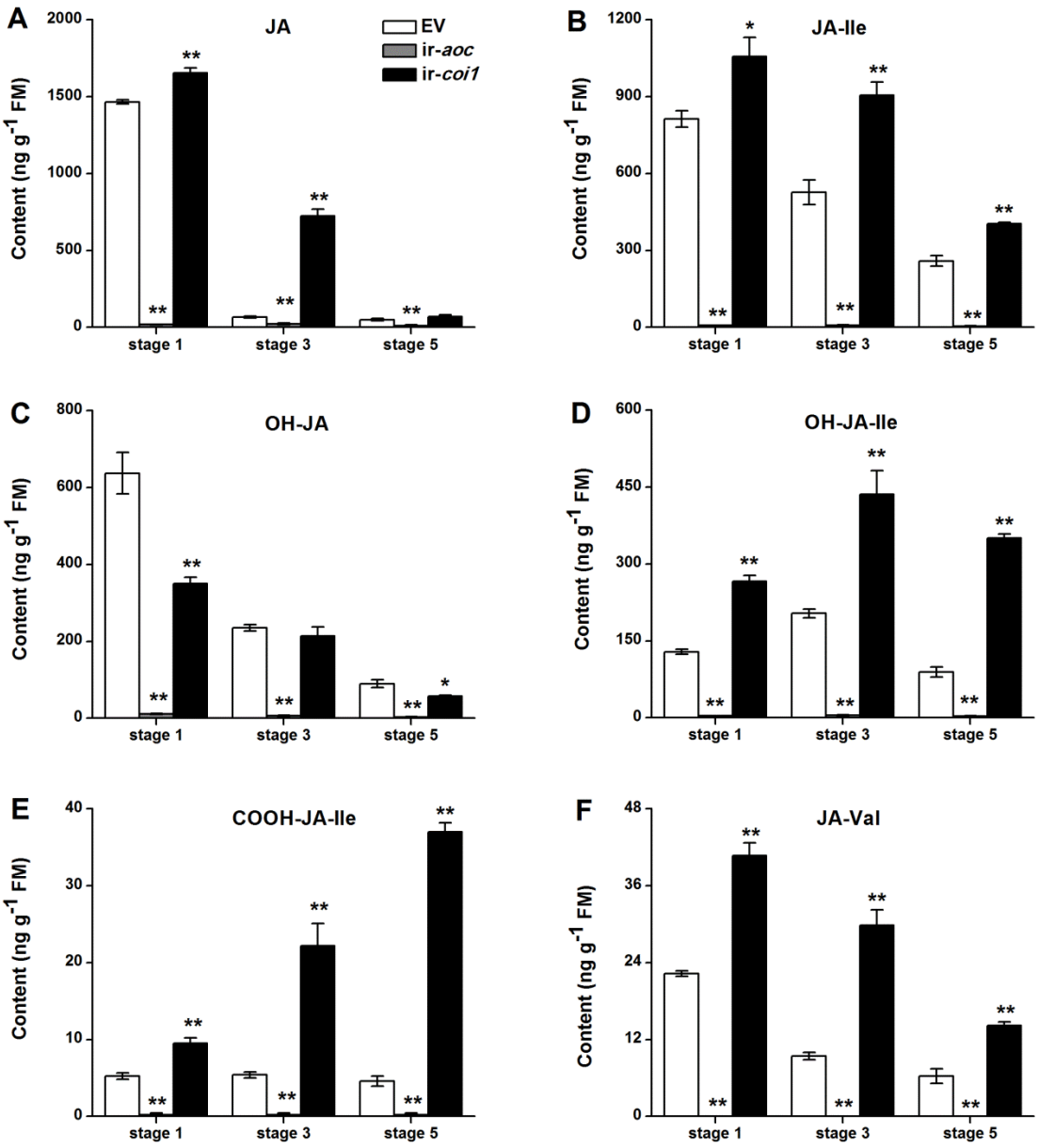

Fig. S1. JA levels in lines deficient in JA biosynthesis (ir-*aoc*) and perception (ir-*coi1*).

Mean JA (A), JA-Ile (B), OH-JA (C), OH-JA-Ile (D), COOH-JA-Ile (E) and JA-Val (F) levels (±SE, n=5) in flowers of EV, ir-*aoc* and ir-*coi1* plants. Samples from three different floral stages were analyzed. Asterisks indicate significant differences in ir-*aoc* or ir-*coi1* compared with control plants (*, $p < 0.05$; **, $p < 0.01$; Student's t-test).

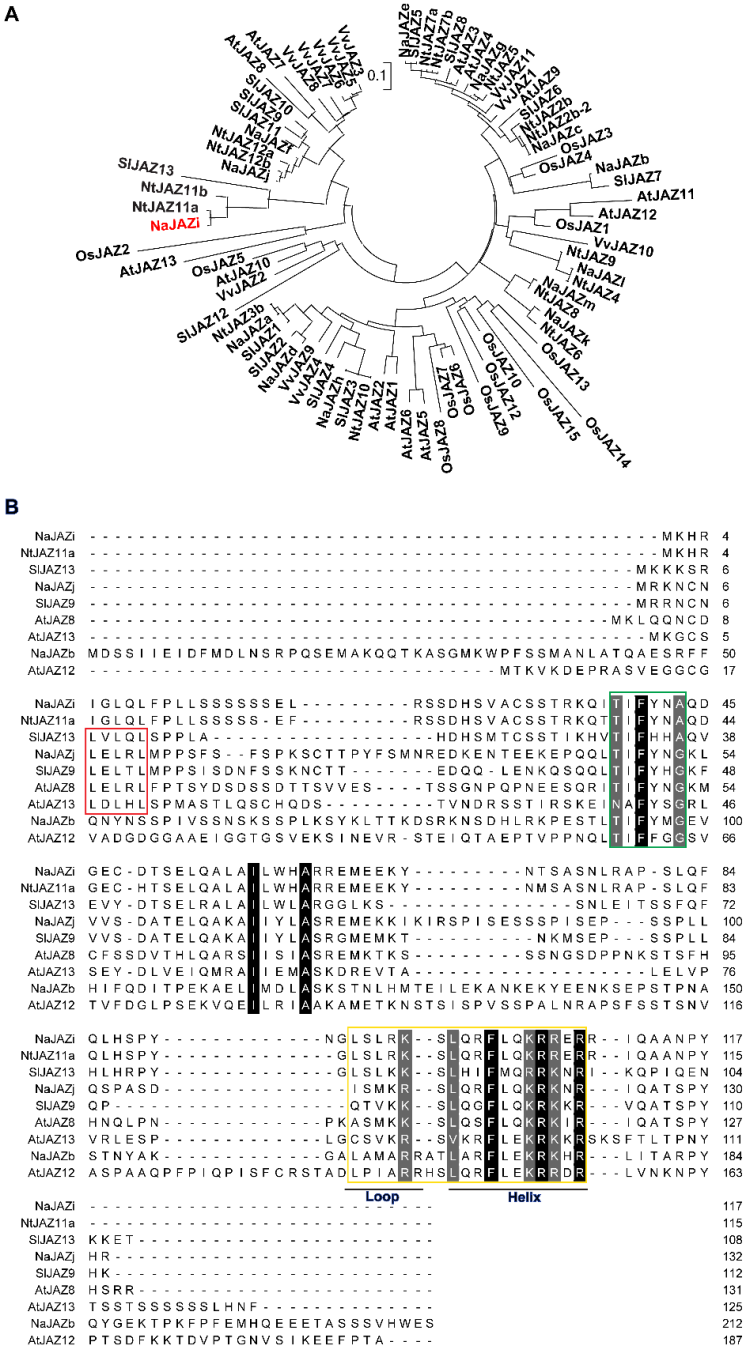

Fig. S2. Phylogenetic analysis and sequence alignment of JAZ genes in different species.

(A) Phylogenetic analysis of JAZ gene family from *N. attenuata* (Na), *Oryza sativa*, (Os), *N. tabacum* (Nt), *Vitis vinfera* (Vv), *Solanum lycopersicum* (Sl) and Arabidopsis (At). (B) Sequence alignment of JAZ genes from different species. EAR motif was highlighted in red box. TIFY domain was highlighted in green box. Jas motif was highlighted in yellow box.

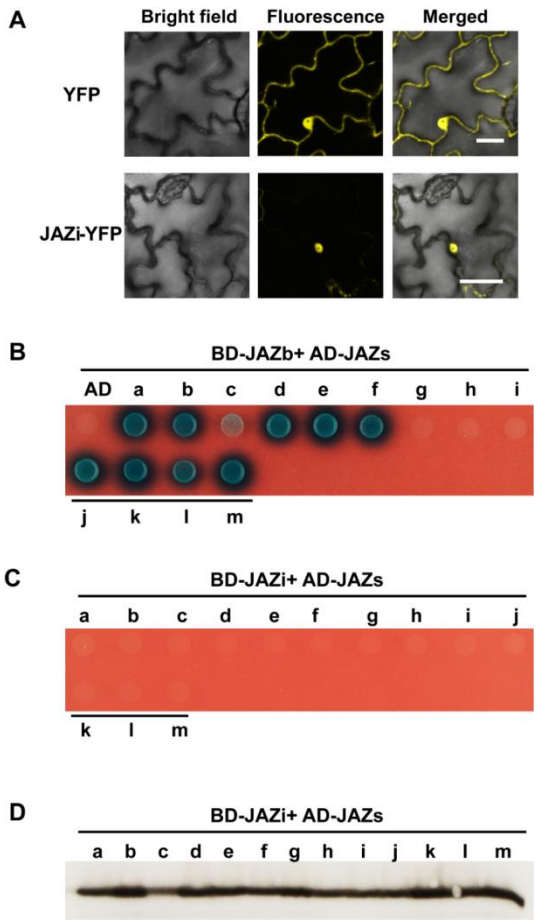

Fig. S3. Subcellular localization of JAZi and JAZ homo-/hetero dimerization. (A) Subcellular localization of NaJAZi. YFP and JAZi-YFP were transiently expressed in *N. attenuata* leaves. After incubation for 48 h, transformed cells were observed under a confocal microscope. The photographs were taken in UV light, visible light, and in combination (merged), respectively. Scale bar, 20 μm. (B) NaJAZb homo- and heterodimerization assay by yeast two-hybrid. BD-JAZs and AD-JAZb were co-transformed into yeast strain Y2Hgold. BD and AD-JAZb co-transformed yeast were used as control. (C) NaJAZi homo- and heterodimerization assays were conducted by yeast two-hybrid assays. BD-JAZs and AD-JAZi were co-transformed into yeast strain Y2Hgold. The transformants were grown on QDO (SD/-Ade/-His/-Leu/-Trp/) plate with 40mg/L X-α-gal. (D) Immunoblot analysis of JAZ proteins in yeast strains used for Y2H assays shown in (C). BD-JAZi fusion protein was detected with anti-myc antibody.

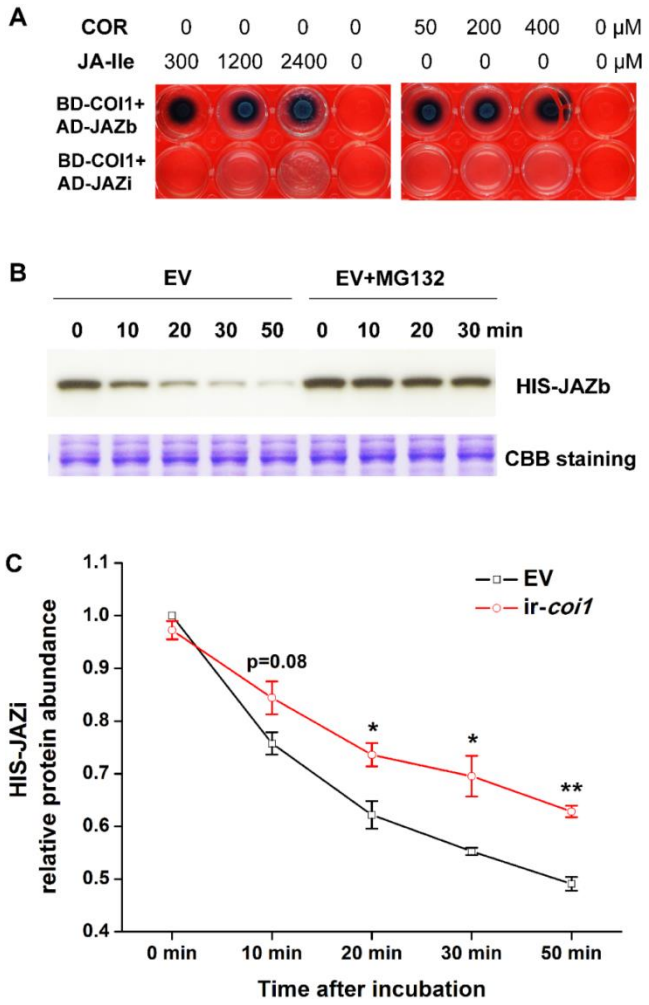

Fig. S4. Interactions between NaCO1 and NaJAZs and *in vitro* NaJAZ degradation assay.

(A) Interactions between NaCOI1 and NaJAZ proteins by yeast two-hybrid assays. GAL4 DNA-binding domain (BD) and activation domain (AD) fusions were co-transformed into yeast strain Y2Hgold. The transformants were grown on QDO (SD/-Ade/-His/-Leu/-Trp/+40mg/L X-α-gal) plates in the presence of coronatine (COR) or JA-Ile or a solvent control. (B) *In vitro* JAZb degradation assays. Purified HIS-JAZb was incubated with total crude extracts from EV and total crude extracts from EV plus MG132. HIS-JAZb was detected using anti-HIS antibody at the indicated incubation time points. The Coomassie Brilliant Blue (CBB) staining is shown as a protein loading control. (C) Mean relative abundance (±SE, n=3) of HIS-JAZi protein levels in different treatments. The relative protein abundance was analyzed by ImageJ software.

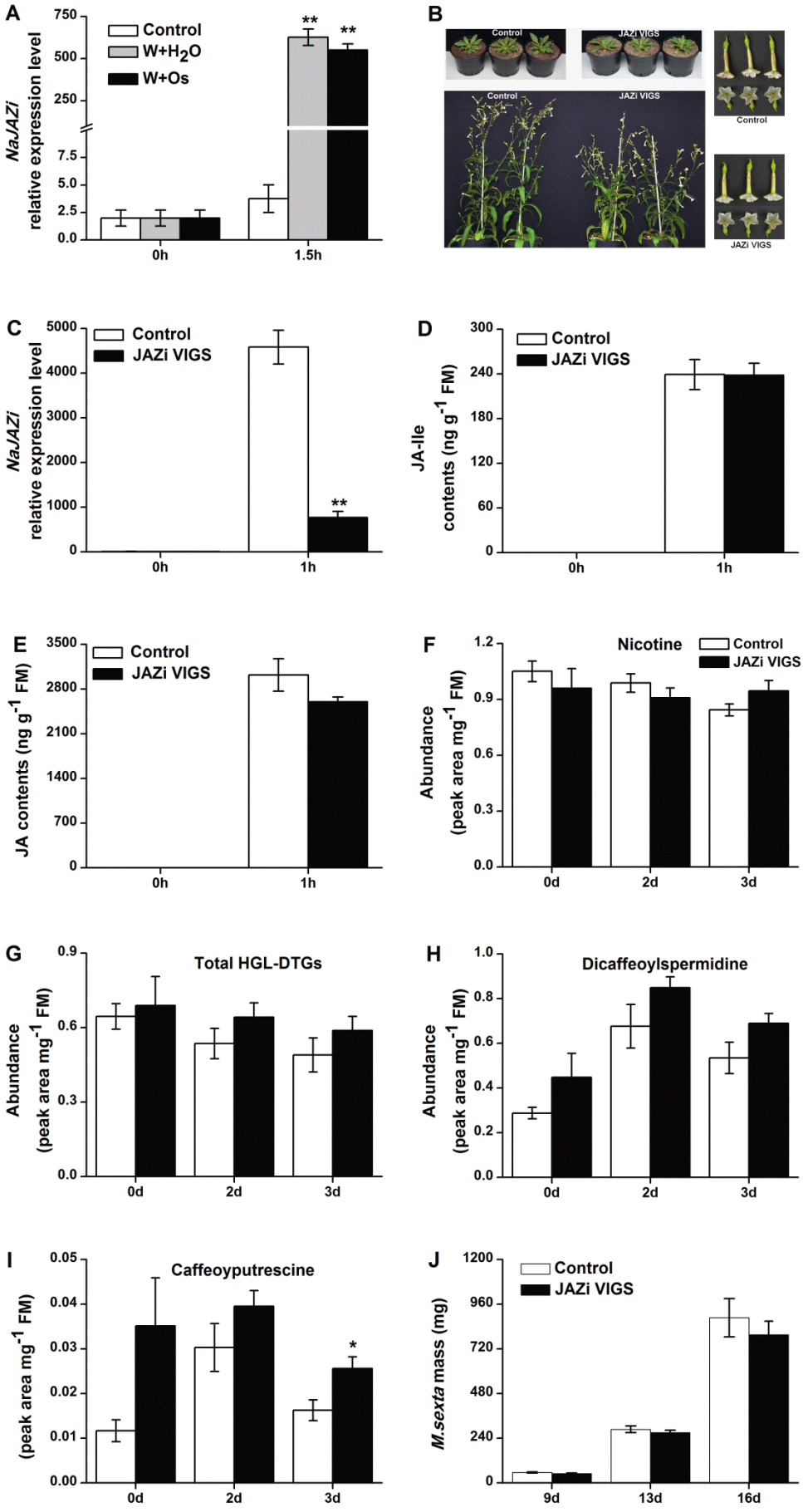
A
NaJAZi relative expression level
Control
W+H2O
W+Os
0h
1.5h
B
Control
JAZi VIGS
C
NaJAZi relative expression level
Control
JAZi VIGS
0h
1h
D
JA-Ile contents (ng g-1 FM)
Control
JAZi VIGS
0h
1h
E
JA contents (ng g-1 FM)
Control
JAZi VIGS
0h
1h
F
Nicotine
Abundance (peak area mg-1 FM)
Control
JAZi VIGS
0d
2d
3d
G
Total HGL-DTGs
Abundance (peak area mg-1 FM)
0d
2d
3d
H
Dicaffeoylspermidine
Abundance (peak area mg-1 FM)
0d
2d
3d
I
Caffeoyputrescine
(peak area mg-1 FM)
0d
2d
3d
J
M.sexta mass (mg)
Control
JAZi VIGS
9d
13d
16d

Fig. S5. Silencing of *NaJAZi* does not affect leaf resistance to *M. sexta* larvae. (A) Mean transcripts levels (±SE, n=5) of NaJAZi in *N. attenuata* leaves after W+R or wounding control (W+H_2O). Transcripts levels were analyzed by RT-qPCR. (B) Growth phenotype of *NaJAZi*-silencing plants. (C) Mean transcript levels (±SE, n=7) of *NaJAZi* in leaves of VIGS control and JAZi VIGS plants after W+R treatment. Transcripts levels were analyzed by RT-qPCR. Mean JA (D) and JA-Ile (E) levels (±SE, n=7) in leaves of VIGS control and JAZi VIGS plants after W+R treatments. Samples were harvested before or 1 h after treatments. Mean nicotine (F), 17-hydroxygeranyllinalool diterpene glycosides (DTGs) (G), caffeoyputrescine (H) and dicaffeoylspermidine (I) levels (±SE, n=7) in leaves of VIGS control and JAZi VIGS plants after W+R treatments. (J) *M. sexta* performance on VIGS control and JAZi VIGS plants. *M. sexta* larva mass (±SE, n=30) was measured at 9, 13 and 16 d after feeding on indicated plants. Asterisks indicate significant differences in JAZi VIGS plants compared with VIGS EV control plants (**, $p < 0.01$; Student's t-test).

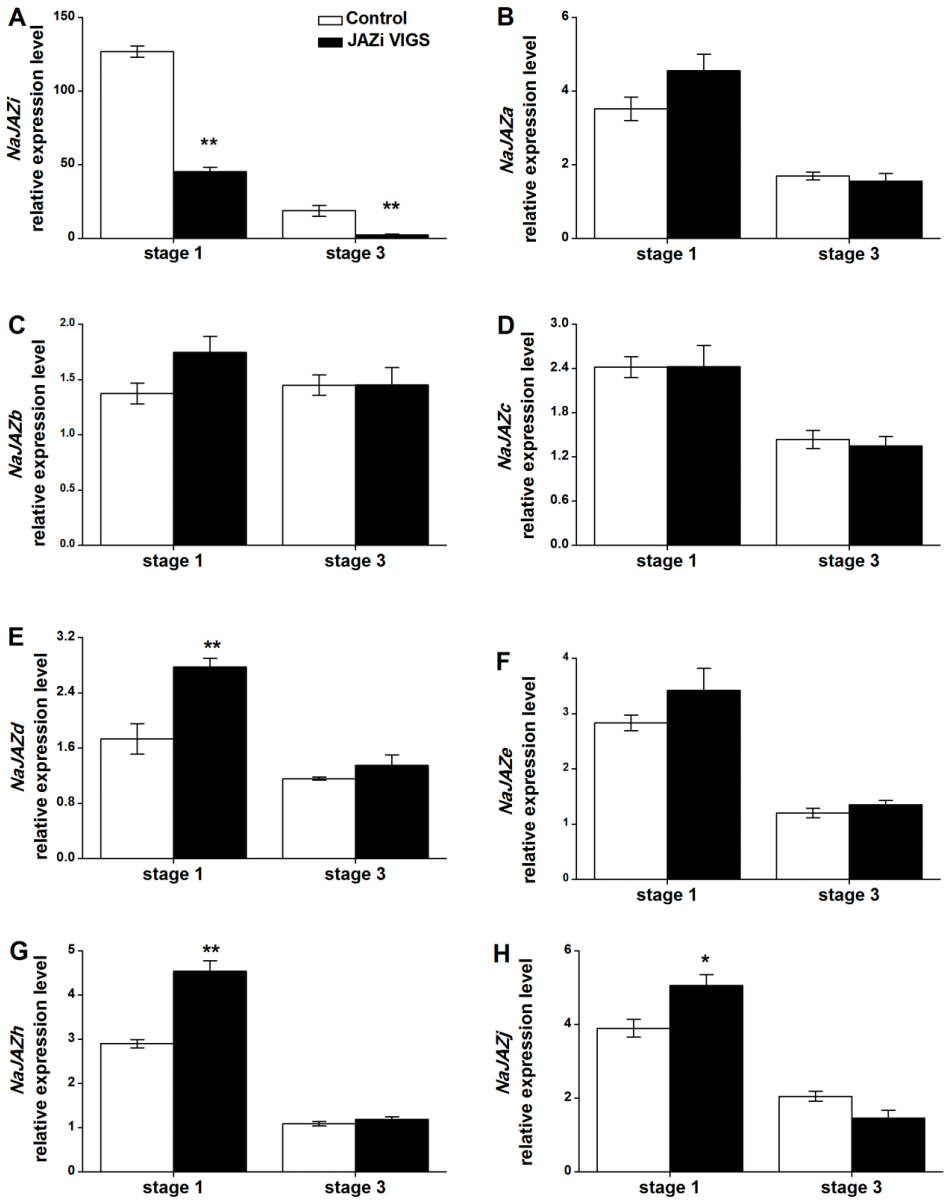

Fig. S6. Transcript abundance of JAZ genes in *NaJAZi*-silenced plants.

Mean transcript levels (±SE, n=5) of *JAZi* (A), *JAZa* (B), *JAZb* (C), *JAZc* (D), *JAZd* (E), *JAZe* (F), *JAZh* (G) and *JAZj* (H) in the flowers of VIGS control and JAZi VIGS plants. Transcripts levels were analyzed by RT-qPCR. Asterisks indicate significant differences in JAZi VIGS plants compared with control plants (*, $p < 0.05$; **, $p < 0.01$; Student's t-test).

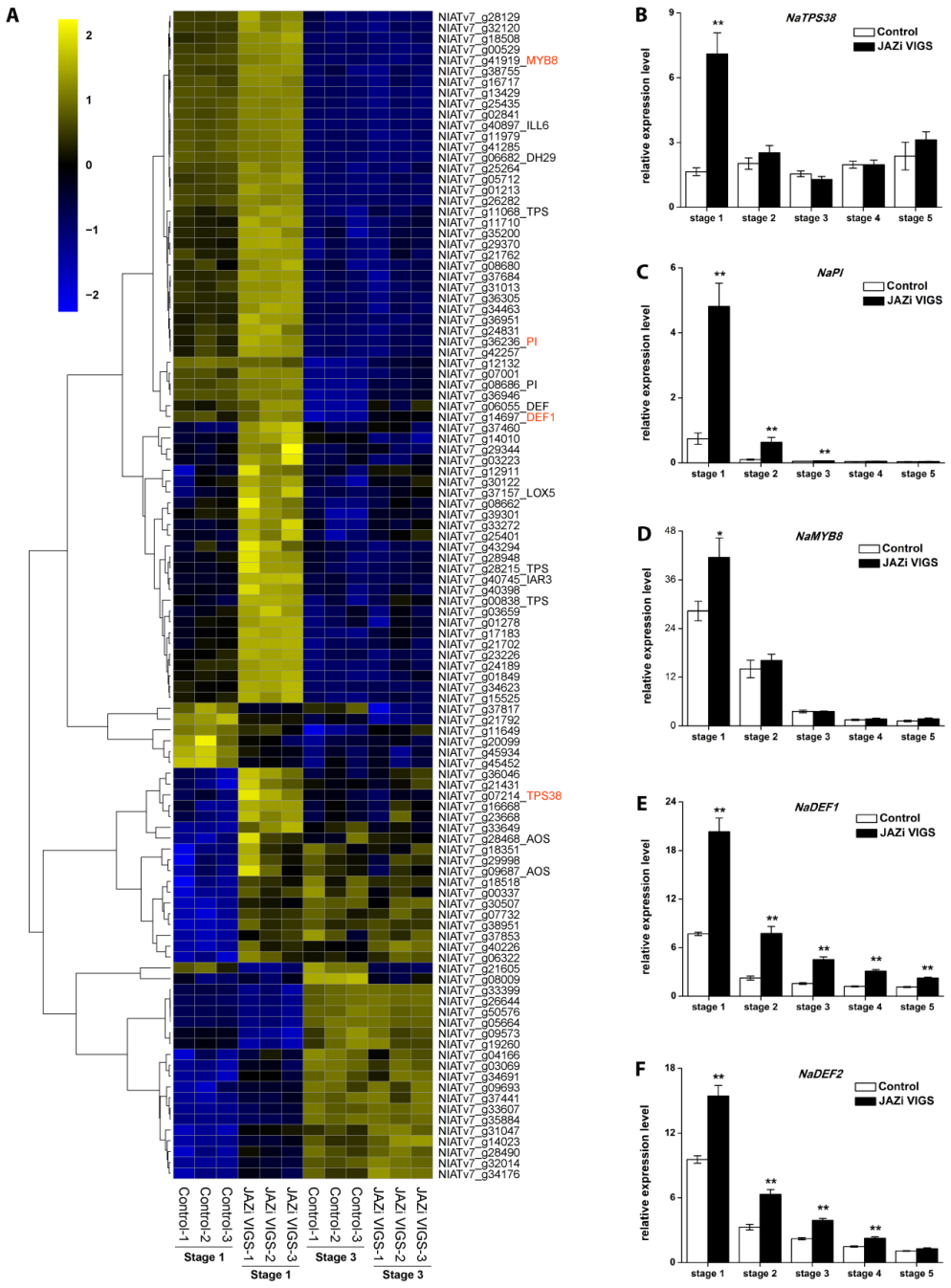

Fig. S7. Up- and down-regulated genes in *NaJAZi*-silenced plants.

Heatmap shows up- and down-regulated genes in JAZi-silencing flowers. The color gradient refers to relative signal abundance. Mean transcript levels (±SE, n=5) of *NaTPS38* (B), *NaPI* (C), *NaMYB8* (D), *NaDEF1* (E) and *NaDEF2* (F) in flowers of VIGS control and JAZi VIGS plants. Transcripts levels were analyzed by RT-qPCR. Asterisks indicate significant differences in JAZi VIGS plants compared with control plants (**, $p < 0.01$; Student's t-test).

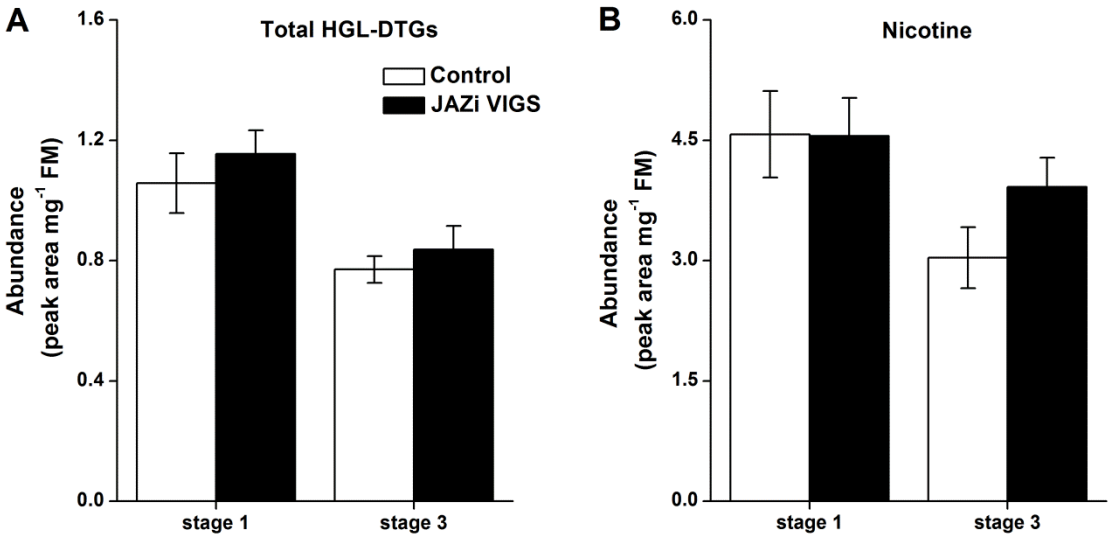

Fig. S8. Silencing of *NaJAZi* does not affect nicotine and DTG levels in developing flowers.

Mean 17-hydroxygeranyllinalool diterpene glycosides (DTGs) (A) and nicotine (B) relative abundance (±SE, n=5) in the flowers of VIGS control and JAZi VIGS plants.

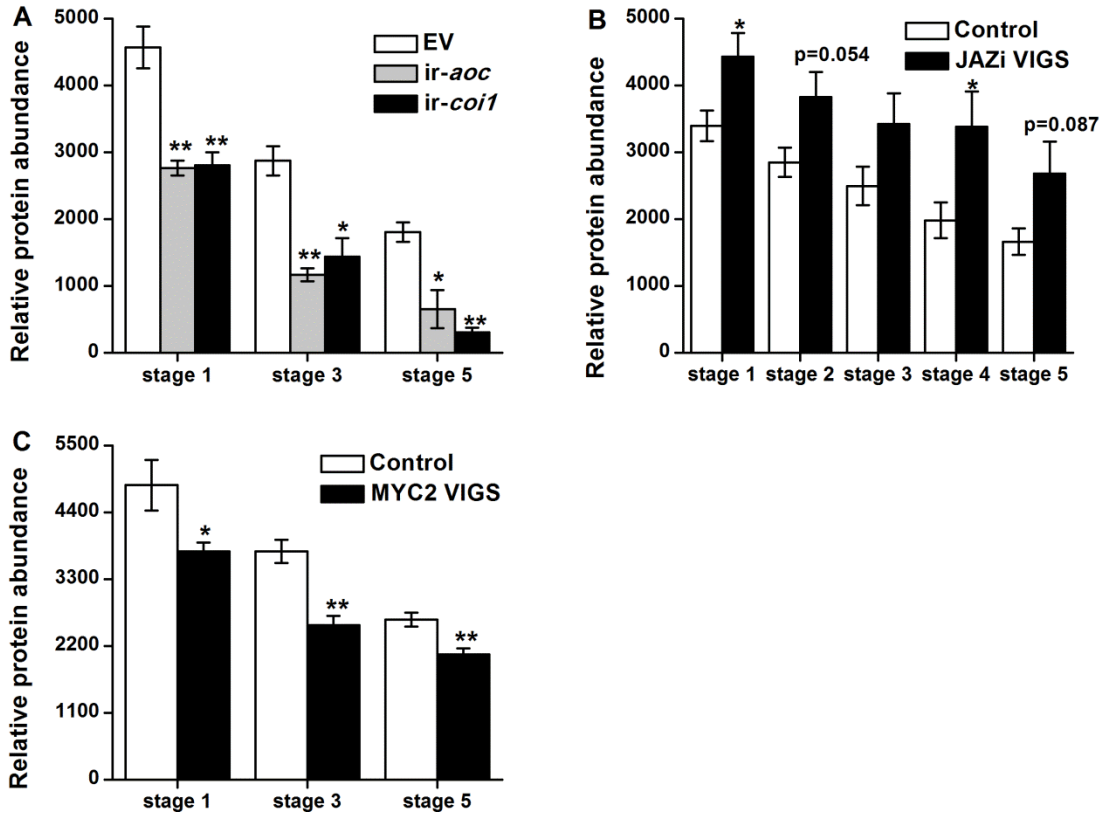

Fig. S9. Relative defensin protein levels in different genotypes.

(A) Mean defensin protein levels (±SE, n=3) in flowers of ir-*aoc*, ir-*coi1* and EV plants (*, $p < 0.05$; **, $p < 0.01$; Student's t-test). (B) Mean defensin protein levels (±SE, n=5) in flowers of VIGS control and JAZi VIGS plants (*, $p < 0.05$; Student's t-test). (C) Mean defensin protein levels (±SE, n=5) in flowers of VIGS control and MYC2 VIGS plants (*, $p < 0.05$; Student's t-test). The relative protein abundance was analyzed by ImageJ software.

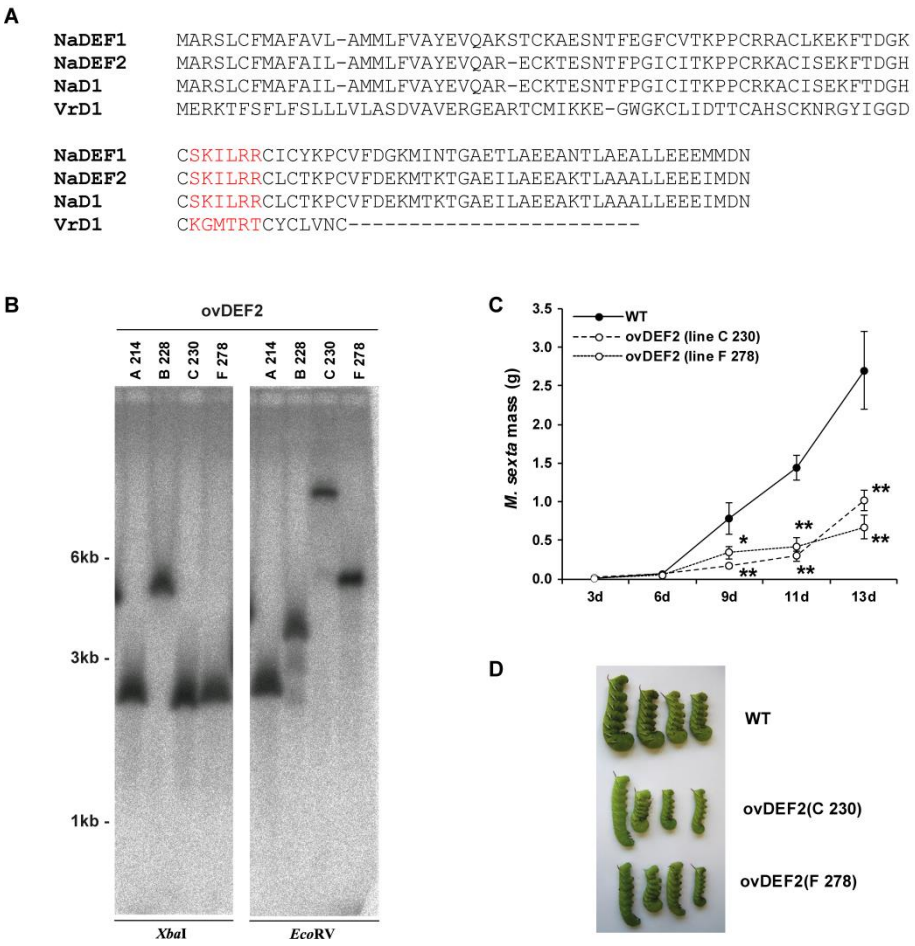

Fig. S10. Ectopic expression of *NaDEF2* in leaves enhances resistance to *M. sexta* larvae.

(A) Alignment analysis of *N. attenuata* NaDEF1, NaDEF2, *N. alata* NaD1 and *V.radiata* VrD1. The putative α-amylase inhibitory activity region is highlighted in red. (B) Southern blot analysis for the determination of T-DNA copy numbers of four independend ov*DEF2* lines. Genomic DNA was isolated from seedlings homozygous to the hygromycin resistance marker and digested in separate reactions with *Xba*I and *Eco*RV. A radiolabeled fragment of the hygromycin resistance marker (*hpt*II) served as probe. (C) *M. sexta* performance on leaves of rosette-stage wild type (WT) and ov*DEF2* plants in the glasshouse. *M. sexta* larval mass was determined 3, 6, 9, 11 and 13 days after infestation (±SE, n = 12 plants). Asterisks indicate statistically significant differences between control and transgenic plants (*, $p < 0.05$; **, $p < 0.01$; Student's t-test). (D) Pictures depict *M. sexta* caterpillars after 13 days of feeding from WT and ov*DEF2* plants.

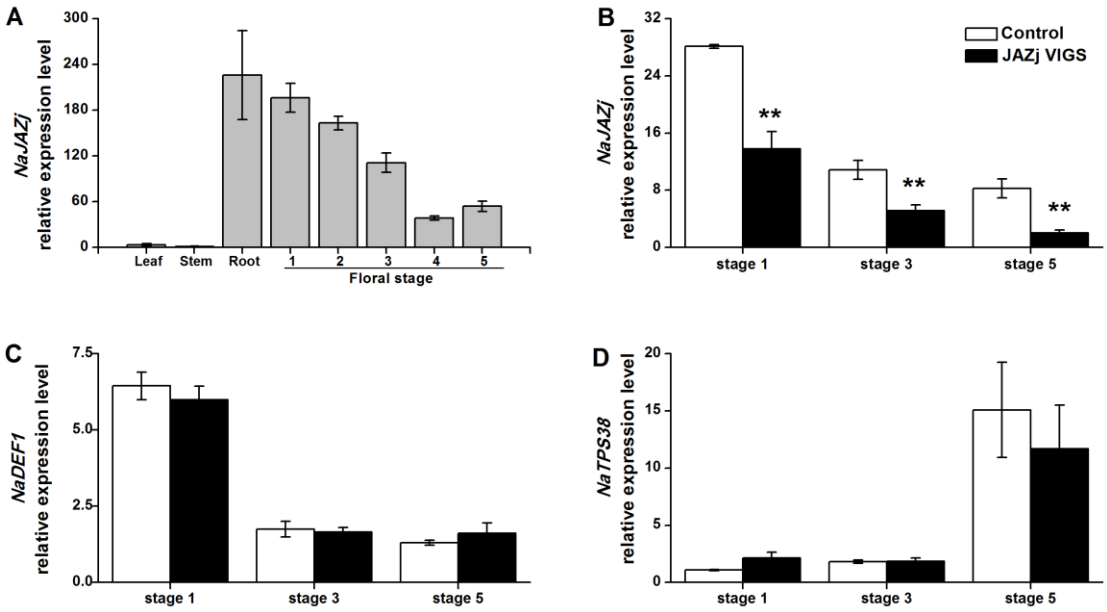

Fig. S11. Silencing of *NaJAZj* does not affect the expression of floral defense-related genes.

Mean transcript levels (±SE, n=5) of *NaJAZj* in different tissues of *N. attenuata*. Transcripts levels were analyzed by RT-qPCR. (B) Mean transcripts levels (±SE, n=4-5) of *NaJAZj* (B), *NaDEF1* (C) and *NaTPS38* (D) in the flowers of VIGS control and JAZj VIGS plants. Transcripts levels were analyzed by RT-qPCR. Asterisks indicate significant differences in NINJA-like VIGS plants compared with control plants (**, $p < 0.01$; Student's t-test).

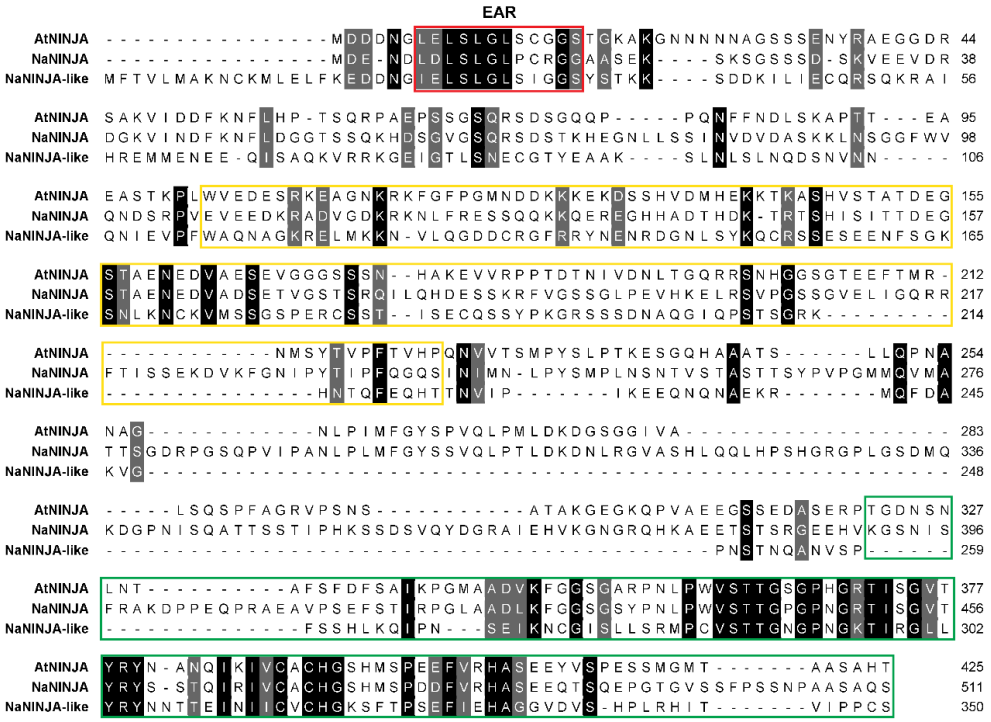

Fig. S12. Alignment analysis of NINJA and NINJA-like.

EAR motif is highlighted in the red box. B domain is highlighted in the yellow box and the C domain is highlighted in the green box.

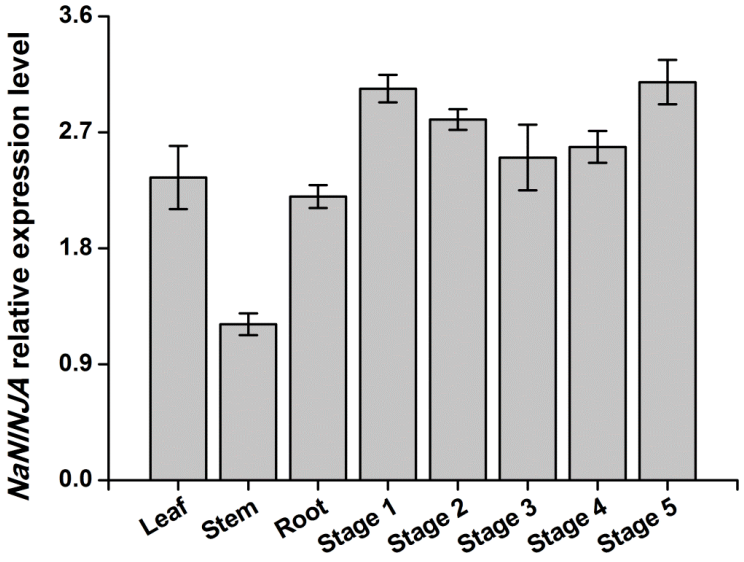

Fig. S13. Transcript accumulations of the *NaNINJA* gene.

Mean transcripts levels (±SE, n=5) of *NaNINJA* in different tissues of *N. attenuata*. Transcripts levels were analyzed by RT-qPCR.

Table S1. The transcripts per million (TPM) values of JAZs from the RNA-seq analysis.

Gene name	Leaf control	Leaf treated	Stem treated	Root treated	Flower bud	Corolla early	Corolla late	Opening flower	Pedicel	Stigma	Nectary	Anther	Ovary
NaJAZa	43.95	1634.56	800.62	344.79	216.39	274.45	104.7	70.56	152.9	138.37	105.83	114.17	108.3
NaJAZb	71.67	431.55	251.72	5.02	24.27	43.09	43.13	20.06	15.24	19.48	2.2	12.91	13.61
NaJAZc	24.4	114.45	69.67	78.99	89.16	67.87	63.8	51.38	72.59	102.1	66.49	21.04	84.32
NaJAZd	7.74	736.5	359.93	78.29	37.15	38.95	47.38	34.15	17.65	47.27	67.33	50.82	53.3
NaJAZe	4.47	9.56	8.46	77.91	23.47	14.52	5.9	8.06	8.31	10.99	12.37	20.86	17.33
NaJAZf	0	151.31	3.5	1.09	1.11	2.59	0.3	0	0	0	0	0.75	0
NaJAZg	0	0	0	51.52	0	0.08	0	0	0.1	0.12	0	0	0
NaJAZh	42.29	740.37	551.18	48.82	74.2	54.96	28.27	17.65	33.64	47.41	30.33	31.28	33.9
NaJAZi	0	0.53	0.29	0.07	157.91	248.72	0.57	1.08	0.25	151.92	8.93	61.48	16.27
NaJAZj	0.59	690.1	219.95	11.69	35.08	35.65	20.26	12.43	3.14	12.08	13.81	40.8	7.78
NaJAZk	1.1	1.74	3.6	2.56	2.21	2.52	4.22	1.72	3.35	2.21	2.63	0.84	3.21
NaJAZl	0	0.17	0.2	0.23	0	0.18	0	0.24	0	0	0	0	0.24
NaJAm	3.71	2.73	9.33	10.93	9.01	7.67	8.58	15.1	6.58	10.5	16.14	6.4	26.73

Table S2. DNA primers used in this study.

Gene	Sequence (5'-3')	Purpose
JAZi-RT-F	TCATTCTGTGGCATGTTCGT	RT-qPCR
JAZi-RT-R	TGAAACTGCAGAGATGGTGC	RT-qPCR
AD/BD-NaJAZi-F	GCCAGCATATGATGAAGCACAGAATTGGCCT	Y2H
AD/BD-NaJAZi-R	TCCATCCCGGGTGGTATGGATTAGCTGCTTGAA	Y2H
AD/BD-NaJAZb-F	GCCAGCATATGATGGATTCAAGTATTATTGA	Y2H
AD/BD-NaJAZb-R	TCAATCCCGGGTGGCTTTCCCAATGAACGCTTG	Y2H
BD-COI1-F	TTCATCATATGATGGAGGAGCGTAGCTCCAC	Y2H
BD-COI1-R	TCCATCCCGGGAATTCAGCGAGAAGGGAATTTG	Y2H
AD-MYC2a-F	CCCAGCATATGATGACGGACTATAGAATACC	Y2H
AD-MYC2a-R	TACAGATCGATGTCGCGATTCAGCAATTCTGG	Y2H
AD-MYC2b-F	CCCAGCATATGATGAATTTGTGGAATACTAG	Y2H
AD-MYC2b-R	TACAGATCGATGGCGTGTTTCAGCAACTCTGG	Y2H
AD/BD-NINJA-F	GCGCGCATATGATGGATGAAAACGATCTTGA	Y2H
AD/BD-NINJA-R	TAAATCCCGGGAAGCTTTGGGCAGAGGCAGCCG	Y2H
AD-NaJAZa-F	GCCAGCATATGATGGCATCATCGGAGATTGT	Y2H
AD-NaJAZa-R	TCCATCCCGGGTGGACGAATTGAATACCTACAC	Y2H
AD-NaJAZc-F	TCAGTCCCGGGTATGGAGAGAGATTTTATGGG	Y2H
AD-NaJAZc-R	TCAATCTCGAGCGGTCTCCTTACCGGCTATCA	Y2H

BD-NaJAZc-F	TCAGTCCATGGAGATGGAGAGAGATTTTATGGG	Y2H
BD-NaJAZc-R	TCAATGTCGAC G GGTCTCCTTACCGGCTATCA	Y2H
AD/BD-NaJAZd-F	GCCAGCATATGATGGGGTTATCGGAGATTGT	Y2H
AD/BD-NaJAZd-R	TCGATCCCGGGTGAAAGAACTGCTCAGTTTTCA	Y2H
AD/BD-NaJAZe-F	GCCAGCATATGATGGGTTTGACTCATCATGT	Y2H
AD/BD-NaJAZe-R	TCAATCCCGGGTGCGTCTCCTTGACCAAATTGA	Y2H
AD/BD-NaJAZf-F	GCCAGCATATGATGAGAAGAAACTGTAACTTG	Y2H
AD/BD-NaJAZf-R	TCGATCCCGGGTGGTGATGATATGGAGAAGTTT	Y2H
AD/BD-NaJAZg-F	GCCAGCATATGATGGAGAGAGATTTCATGGG	Y2H
AD/BD-NaJAZg-R	TCGATCCCGGGTGTATAGTAGCAGGAAGAACAG	Y2H
AD/BD-NaJAZh-F	GCCCGCATATGATGTCAAATTCGCAAAATTC	Y2H
AD/BD-NaJAZh-R	TCGGTCCCGGGTGTAACTTGAAATTGAGATCGA	Y2H
AD/BD-NaJAZj-F	GCCCGCATATGATGAGAAAAAACTGTAACTT	Y2H
AD/BD-NaJAZj-R	TCATTCCCGGGTGGCGATGATAAGGAGAAGTTG	Y2H
AD/BD-NaJAZk-F	GACAGCATATGATGCCGCCGGAAGAATCAGT	Y2H
AD/BD-NaJAZk-R	TAGGTCCCGGGTGCCTGTCTTTTCGCTTCTCAA	Y2H
AD/BD-NaJAZl-F	GCCCGCATATGATGTATTGCAGCTCCAAAGT	Y2H
AD/BD-NaJAZl-R	CAGGTCCCGGGTGACTATTCTTTTCCTTCAAAC	Y2H
AD/BD-NaJAZm-F	GCCAGCATATGATGGCGCCGGAAGAAACAGT	Y2H
AD/BD-NaJAZm-R	TCCATCCCGGGTGCTCTTTGGCATCTTTGTCAT	Y2H
AD-TOPLESS-F	CCGCAGAATTCATGTCATCTCTCAGCAGAGA	Y2H
AD-TOPLESS-R	AATCAGGATCCCTCTTGGTGCTTGTTCGGAGC	Y2H
AD/BD-NINJA-like-F	CCGCAGAATTCATGTTTACTGTGTTAATGGC	Y2H
AD/BD-NINJA-like-R	AATCAGGATCCCAGAACAAGGGGGGATTACAG	Y2H
TOPO-NINJA-like-F	CACCATGTTTACTGTGTTAATGGC	pENTR
TOPO-NINJA-like-R	AGAACAAGGGGGGATTACAG	pENTR
TOPO-JAZi-F	CACCATGGGCTGTCCCTAAGAAAA	pENTR
TOPO-JAZi-R	ACAGGTGATCCAACCTTCCA	pENTR
NINJA-like-RT-F	GCTCAGAATGCTGGGAAAAG	RT-qPCR
NINJA-like-RT-R	CATCTTTCCGGTGAACCACT	RT-qPCR
TPS38-RT-F	ATGGGCTGTTGGTTTCACT	RT-qPCR
TPS38-RT-R	TGCATTGATGTCCCATCTGT	RT-qPCR
PI-RT-F	ACACGAGACTTGGGAAATGG	RT-qPCR
PI-RT-R	GTGTCCCTGGAAAACCTTCA	RT-qPCR
MYB8-RT-F	ACCGGGACGAACAGATAATG	RT-qPCR
MYB8-RT-R	CGACGAAGAATTTGGGTGTT	RT-qPCR
DEF2-RT-F	TGCATTACCAAACCACCTTG	RT-qPCR
DEF2-RT-R	CAGCCAAAGTTTTTGCTTCC	RT-qPCR
DEF1-RT-F	ACATTCGAGGGATTCTGCGT	RT-qPCR

DEF1-RT-R	TCCTCGGCTAAAGTTTCAGCT	RT-qPCR
NINJA-RT-F	ATCTACCGTGGGTCTCAACG	RT-qPCR
NINJA-RT-R	AGTTTGCTCTTCGCTTGCAT	RT-qPCR
JAZa-RT-F	ATGACGATATTCTACGGCGG	RT-qPCR
JAZa-RT-R	TAAGTGAAGCTCGTCTCGCA	RT-qPCR
JAZb-RT-F	ACACCAAATGCATCCACAAA	RT-qPCR
JAZb-RT-R	GACGCCGTTTCTTCTTCTTG	RT-qPCR
JAZc-RT-F3	TACCTGCCTCAGGTCATTCC	RT-qPCR
JAZc-RT-R3	GGAACCGCTGCTGACATTAT	RT-qPCR
JAZd-RT-F	ACCGCAGTTTTGAACCAACT	RT-qPCR
JAZd-RT-R	ATTTGCCTTAGCTGCTGGAA	RT-qPCR
JAZe-RT-F	CGCACTACACGTCGACAACT	RT-qPCR
JAZe-RT-R	CAGCGCTGTTAGTTGGAACA	RT-qPCR
JAZh-RT-F	TCGAATTTCGTGCAGACTTG	RT-qPCR
JAZh-RT-R	TACAGCACTCTGACGAACGG	RT-qPCR
JAZj-RT-F	AGCTCAGGCTTATGCCTCCT	RT-qPCR
JAZj-RT-R	TCTGAAATTGGTGACCGGAT	RT-qPCR
MYC2a-RT-F	GGCCCGGAACAACTACTACA	RT-qPCR
MYC2a-RT-R	CCCCGTCGATTAAAGTCTGA	RT-qPCR
MYC2b-RT-F	TCTGGTGCGATGAAGTCAAG	RT-qPCR
MYC2b-RT-R	CTGCTTCGACGTGATTCAAA	RT-qPCR
JAZj-VIGS-F	TCATCACTAGTCCACAGCAGCTAACAATATT	VIGS
JAZj-VIGS-R	ATCTCCCCGGGCAAAATATATGTACAAATGG	VIGS
MYC2a-VIGS-F	CCAGCACTAGTATCAAGAGGTAGCAACGATG	VIGS
MYC2a-VIGS-R	ACTTTCCCGGGGACACATTTGGTACAACAGC	VIGS
MYC2b-VIGS-F	CCAGCACTAGTATGAATTTGTGGAATACTAG	VIGS
MYC2b-VIGS-R	ACTTTCCCGGGGGCATAGGTCCATGTCTCGC	VIGS
JAZi-VIGS-F	TCATCACTAGTATCACAATTTTCTACAACG	VIGS
JAZi-VIGS-R	ATCTCCCCGGGGAAGTATCCGCATATCGCAAA	VIGS
NINJA-like-VIGS-F	CACGCGGATCCATGTTTACTGTGTTAATGGC	VIGS
NINJA-like-VIGS-R	CCCGCATCGATTTGATTCAAAGAAAGATTCA	VIGS

Table S3. Gene accession numbers used in this study

Name	Species	Accession number

AtAFP1	*Arabidopsis*	AT1G69260
AtAFP2	*Arabidopsis*	AT1G13740
AtAFP3	*Arabidopsis*	AT3G29575
AtAFP4	*Arabidopsis*	AT3G02140
AtNINJA	*Arabidopsis*	AT4G28910
AtJAZ1	*Arabidopsis*	AT1G19180
AtJAZ2	*Arabidopsis*	AT1G74950
AtJAZ3	*Arabidopsis*	AT3G17860
AtJAZ4	*Arabidopsis*	AT1G48500
AtJAZ5	*Arabidopsis*	AT1G17380
AtJAZ6	*Arabidopsis*	AT1G72450
AtJAZ7	*Arabidopsis*	AT2G34600
AtJAZ8	*Arabidopsis*	AT1G30135
AtJAZ9	*Arabidopsis*	AT1G70700
AtJAZ10	*Arabidopsis*	AT5G13220
AtJAZ11	*Arabidopsis*	AT3G43440
AtJAZ12	*Arabidopsis*	AT5G20900
AtJAZ13	*Arabidopsis*	AT3G22275
OsJAZ1	*Oryza sativa*	Os04g55920
OsJAZ2	*Oryza sativa*	Os07g05830
OsJAZ3	*Oryza sativa*	Os08g33160
OsJAZ4	*Oryza sativa*	Os09g23660
OsJAZ5	*Oryza sativa*	Os04g32480
OsJAZ6	*Oryza sativa*	Os03g28940
OsJAZ7	*Oryza sativa*	Os07g42370
OsJAZ8	*Oryza sativa*	Os09g26780
OsJAZ9	*Oryza sativa*	Os03g08310
OsJAZ10	*Oryza sativa*	Os03g08330
OsJAZ11	*Oryza sativa*	Os03g08320
OsJAZ12	*Oryza sativa*	Os10g25290
OsJAZ13	*Oryza sativa*	Os10g25230
OsJAZ14	*Oryza sativa*	Os10g25250
OsJAZ15	*Oryza sativa*	Os03g27900
NtJAZ2b	*N. tabacum*	KC246550
NtJAZ2b-2	*N. tabacum*	KC246551
NtJAZ3b	*N. tabacum*	KC246552
NtJAZ4	*N. tabacum*	KC246553
NtJAZ5	*N. tabacum*	KC246554
NtJAZ6	*N. tabacum*	KC246555
NtJAZ7a	*N. tabacum*	KC246556

NtJAZ7b	*N. tabacum*	KC246557
NtJAZ8	*N. tabacum*	KC246558
NtJAZ9	*N. tabacum*	KC246559
NtJAZ10	*N. tabacum*	KC246560
NtJAZ11a	*N. tabacum*	KC246561
NtJAZ11b	*N. tabacum*	KC246562
NtJAZ12a	*N. tabacum*	KC246563
NtJAZ12b	*N. tabacum*	KC246564
VvJAZ1	*Vitis vinfera*	XM-002284819
VvJAZ2	*Vitis vinfera*	XM-002262714
VvJAZ3	*Vitis vinfera*	XM-003634778
VvJAZ4	*Vitis vinfera*	XM-002272327
VvJAZ5	*Vitis vinfera*	XM-002277733
VvJAZ6	*Vitis vinfera*	XM-002277769
VvJAZ7	*Vitis vinfera*	XM-002277916
VvJAZ8	*Vitis vinfera*	CBI30922
VvJAZ9	*Vitis vinfera*	XM-002277121
VvJAZ10	*Vitis vinfera*	XM-002263220
VvJAZ11	*Vitis vinfera*	XM-002282652
SlJAZ1	*Solanum lycopersicum*	Solyc07g042170
SlJAZ2	*Solanum lycopersicum*	Solyc12g009220
SlJAZ3	*Solanum lycopersicum*	Solyc03g122190
SlJAZ4	*Solanum lycopersicum*	Solyc12g049400
SlJAZ5	*Solanum lycopersicum*	Solyc03g118540
SlJAZ6	*Solanum lycopersicum*	Solyc01g005440
SlJAZ7	*Solanum lycopersicum*	Solyc11g011030
SlJAZ8	*Solanum lycopersicum*	Solyc06g068930
SlJAZ9	*Solanum lycopersicum*	Solyc08g036640
SlJAZ10	*Solanum lycopersicum*	Solyc08g036620
SlJAZ11	*Solanum lycopersicum*	Solyc08g036660
SlJAZ12	*Solanum lycopersicum*	Solyc01g009740
SlJAZ13	*Solanum lycopersicum*	LOC104649733